NUMERICAL LINEAR ALGEBRA WITH APPLICATIONS
Numer. Linear Algebra Appl. 2010; **00**:1–43
Published online in Wiley InterScience (www.interscience.wiley.com). DOI: 10.1002/nla

Local Fourier analysis of block-structured multigrid relaxation schemes for the Stokes equations

Yunhui He [1], Scott P. MacLachlan[1]

[1] *Department of Mathematics and Statistics, Memorial University of Newfoundland, St. John's, NL A1C 5S7, Canada*

SUMMARY

Multigrid methods that use block-structured relaxation schemes have been successfully applied to several saddle-point problems, including those that arise from the discretization of the Stokes equations. In this paper, we present a local Fourier analysis (LFA) of block-structured relaxation schemes for the staggered finite-difference discretization of the Stokes equations to analyze their convergence behavior. Three block-structured relaxation schemes are considered: distributive relaxation, Braess-Sarazin relaxation, and Uzawa relaxation. In each case, we consider variants based on weighted Jacobi relaxation, as is most suitable for parallel implementation on modern architectures. From this analysis, optimal parameters are proposed, and we compare the efficiency of the presented algorithms with these parameters. Finally, some numerical experiments are presented to validate the two-grid and multigrid convergence factors. Copyright © 2010 John Wiley & Sons, Ltd.

Received ...

KEY WORDS: Local Fourier analysis, staggered finite-difference method (MAC scheme), Stokes equations, distributive relaxation, Braess-Sarazin relaxation, Uzawa relaxation, multigrid

1. INTRODUCTION

Large linear systems of saddle-point type arise in a wide variety of applications throughout computational science and engineering. Such linear systems represent a significant challenge for computation owing to their indefiniteness and often poor spectral properties. Saddle-point problems are well-known and well-studied in numerical analysis [1–3]. Discretization of the Stokes equations naturally leads to saddle-point systems, and solvers for the Stokes equations are a natural first step in developing new algorithms for the Navier-Stokes equations and other saddle-point problems. Two main families of preconditioners are found in the literature for saddle-point systems, such as the Stokes equation. Block preconditioners (cf. [3] and the references therein) are commonly used, since they can easily be constructed from standard multigrid algorithms for scalar elliptic PDEs, such as algebraic multigrid [4]. Monolithic multigrid methods, that are applied directly to the system in coupled form, are potentially more difficult to construct and analyse, since standard pointwise relaxation schemes cannot be applied. Several families of relaxation schemes have, however, been developed for monolithic multigrid methods for the Stokes equations and more complicated saddle-point systems and have been shown to outperform block precondtioners in some cases (see, e.g., [5]). Distributive relaxation [6–8] was the first to be proposed, using a distributive

*Correspondence to: Department of Mathematics and Statistics, Memorial University of Newfoundland, St. John's, NL A1C 5S7, Canada. E-mail:yunhui.he@mun.ca

Contract/grant sponsor: This work was partially supported by an NSERC discovery grant to SM.

operator to allow use of pointwise relaxation schemes on transformed variables. A strongly coupled relaxation scheme was introduced by Vanka [9], based on solving a sequence of localized saddle-point problems in a block overlapping Gauss-Seidel iteration. Two further families are based on using block preconditioning strategies as relaxation schemes, yielding the Braess-Sarazin [10] and Uzawa [11] approaches. Each of these families has been further developed in recent years, including Braess-Sarazin-type relaxation schemes [5,10,12–14], Vanka-type relaxation schemes [5,9,13–18], Uzawa-type relaxation schemes [19–22], distributive relaxation schemes [23,24] and other types of methods [25,26]. The aim of this paper is to analyse block-structured relaxation schemes, including distributive, Braess-Sarazin, and Uzawa relaxation.

Existing analysis of these relaxation schemes leaves several open questions. For finite-element discretizations, variational analysis techniques have been developed for both Braess-Sarazin [27] and Uzawa [19] relaxation. Local Fourier analysis(LFA) has been applied to all of the standard relaxation schemes, including distributive relaxation [28], Vanka relaxation [15, 17], and Braess-Sarazin and Uzawa-type schemes [20, 29]. However, the vast majority of the existing LFA has been for relaxation schemes using (symmetric) Gauss-Seidel approaches. Here, in contrast, we focus on schemes that make use of weighted Jacobi relaxation. Considering modern many-core and accelerated parallel architectures, proper understanding of such schemes is critical to achieving excellent parallel and algorithmic scalability.

Supporting numerical results demonstrate some key conclusions of this analysis. First, distributive weighted-Jacobi relaxation retains the well-known advantages of distributive Gauss-Seidel. This fact, coupled with the low cost per iteration and fine-scale parallelism, recommends this relaxation scheme, at least in the context of the finite-difference scheme considered herein. For Braess-Sarazin relaxation, we find that there is no degradation in predicated multigrid performance for the inexact variant of the algorithm introduced in [27] over the exact variant originally proposed in [10,12]. The same is not true for Uzawa relaxation, where our results show a notable gap between the predicated performance with exact inversion of the resulting approximate Schur complement vs that with only inexact inversion. Furthermore, we see that the assumptions made in [20] for algebraic analysis of Uzawa-type relaxation are sufficient but not necessary for convergence.

In this paper, we consider these three families of relaxation schemes in terms of the computational work and the optimal smoothing factors obtained. The results show that Braess-Sarazin relaxation provides better smoothing than Uzawa in the case of finite-difference discretization. This is in contrast to results in [19] for finite-element discretizations. The gap between finite-difference discretization and finite-element discretization using Braess-Sarzin relaxation is a question for our future work. However, we also see that distributive weighted Jacobi can match the performance of Braess-Sarazin, as has been seen for Gauss-Seidel based relaxation. Extending this analysis to the finite-element case is also a topic for future research.

The outline of the paper is as follows. In Section 2, we introduce the Marker and Cell (MAC) finite-difference discretization of the Stokes equations in two dimensions and some definitions of local Fourier analysis. In Section 3, we present the distributive weighted-Jacobi relaxation schemes and the optimal smoothing factor is given by local Fourier analysis. In Section 4, local Fourier analysis is developed for Braess-Sarazin-type relaxation and optimal parameters are derived. In Section 5, we apply LFA to Uzawa-type relaxation to determine the optimal smoothing factor. Furthermore, a comparison of the relaxation schemes is given. Section 6 presents some experimentally measured two-grid and multigrid convergence factors to confirm the theoretical results. Conclusions are drawn in Section 7.

2. DISCRETIZATION AND LOCAL FOURIER ANALYSIS

2.1. Staggered finite-difference discretization of the Stokes equations

We consider the Stokes equations,

$$-\triangle \boldsymbol{\mathcal{U}} + \nabla p = \boldsymbol{\mathcal{F}}, \quad (1)$$
$$\nabla \cdot \boldsymbol{\mathcal{U}} = 0, \quad (2)$$

for velocity vector, $\boldsymbol{\mathcal{U}} = \begin{pmatrix} u \\ v \end{pmatrix}$, and scalar pressure, p, of a viscous fluid. Discretization of (1) and (2) typically leads to a linear system of the form

$$Kx = \begin{pmatrix} A & B^T \\ B & 0 \end{pmatrix} \begin{pmatrix} \boldsymbol{\mathcal{U}}_h \\ p_h \end{pmatrix} = \begin{pmatrix} \boldsymbol{\mathcal{F}}_h \\ 0 \end{pmatrix} = b, \quad (3)$$

where A corresponds to the discretized vector Laplacian, B is the negative of the discrete divergence operator, and $\boldsymbol{\mathcal{U}}_h = \begin{pmatrix} u_h \\ v_h \end{pmatrix}$.

In this paper, we consider the standard staggered finite-difference discretization in two-dimensions, known as the Marker-and-cell (MAC) scheme (see [30, 31]). The discrete pressure unknowns p_h are defined at cell centres ($\times$-points in Figure 1). The discrete values of u_h and v_h are located at the grid cell faces in the $\circ$- and $\bullet$-points, respectively, see Figure 1.

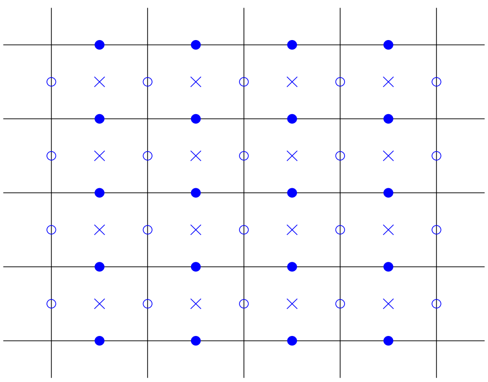

Figure 1. The staggered location of unknowns on mesh $\mathbf{G}_h$: $\times - p, \circ - u, \bullet - v$

The discrete momentum equations read (see [30])

$$-\triangle_h u_h + (\partial_x)_{h/2}\, p_h = F_{1,h}, \qquad -\triangle_h v_h + (\partial_y)_{h/2}\, p_h = F_{2,h},$$

where $\boldsymbol{\mathcal{F}}_h = \begin{pmatrix} F_{1,h} \\ F_{2,h} \end{pmatrix}$. Here, we use the standard five-point discretization for $-\triangle_h$ (for u_h on the $\circ$ grid and for v_h on the $\bullet$ grid) and the approximations

$$(\partial_x)_{h/2}\, p_h(x,y) = \frac{1}{h}\Big(p_h\big(x+h/2,y\big) - p_h\big(x-h/2,y\big)\Big),$$
$$(\partial_y)_{h/2}\, p_h(x,y) = \frac{1}{h}\Big(p_h\big(x,y+h/2\big) - p_h\big(x,y-h/2\big)\Big).$$

The discrete conservation of mass equation is given by

$$(\partial_x)_{h/2}\, u_h(x,y) + (\partial_y)_{h/2}\, v_h(x,y) = 0.$$

We consider uniform meshes with: $h_x = h_y = h$ in this paper.

DOI: 10.1002/nla

2.2. *Definitions and notations*

In order to describe LFA for staggered grids, we first introduce some terminology. More details can be found in [30]. We consider two-dimensional infinite uniform grids $\mathbf{G}_h = \mathbf{G}_h^1 \bigcup \mathbf{G}_h^2 \bigcup \mathbf{G}_h^3$ with

$$\mathbf{G}_h^j = \left\{ \boldsymbol{x}_{k_1,k_2}^j := (k_1,k_2)h + \delta^j, (k_1,k_2) \in \mathbb{Z}^2 \right\}, \text{with } \delta^j = \begin{cases} (0,h/2) & \text{if } \quad j=1, \\ (h/2,0) & \text{if } \quad j=2, \\ (h/2,h/2) & \text{if } \quad j=3, \end{cases}$$

and Fourier functions $\varphi(\boldsymbol{\theta}, \boldsymbol{x}_{k_1,k_2}) \in \text{span}\left\{\varphi_1(\boldsymbol{\theta}, \boldsymbol{x}_{k_1,k_2}), \varphi_2(\boldsymbol{\theta}, \boldsymbol{x}_{k_1,k_2}), \varphi_3(\boldsymbol{\theta}, \boldsymbol{x}_{k_1,k_2})\right\}$ on $\mathbf{G}_h$, in which

$$\begin{aligned} \varphi_1(\boldsymbol{\theta}, \boldsymbol{x}_{k_1,k_2}) &= \begin{pmatrix} e^{i\boldsymbol{\theta}\cdot\boldsymbol{x}_{k_1,k_2}^1/h} & 0 & 0 \end{pmatrix}^T, \ \varphi_2(\boldsymbol{\theta}, \boldsymbol{x}_{k_1,k_2}) = \begin{pmatrix} 0 & e^{i\boldsymbol{\theta}\cdot\boldsymbol{x}_{k_1,k_2}^2/h} & 0 \end{pmatrix}^T, \\ \varphi_3(\boldsymbol{\theta}, \boldsymbol{x}_{k_1,k_2}) &= \begin{pmatrix} 0 & 0 & e^{i\boldsymbol{\theta}\cdot\boldsymbol{x}_{k_1,k_2}^3/h} \end{pmatrix}^T, \ \boldsymbol{\theta} = (\theta_1, \theta_2), \end{aligned}$$

where T denotes the (non-conjugate) transpose of the row vectors. Since $\varphi(\boldsymbol{\theta}, \boldsymbol{x}_{k_1,k_2})$ is periodic in $\boldsymbol{\theta}$ with period 2π, we consider the domain $\boldsymbol{\theta} \in \left[-\frac{\pi}{2}, \frac{3\pi}{2}\right)^2$.

Let L_h be a Toeplitz operator acting on one of the components of $\mathbf{G}_h$

$$\begin{aligned} L_h &\triangleq [s_{\boldsymbol{\kappa}}]_h \ (\boldsymbol{\kappa} = (\kappa_1, \kappa_2) \in \mathbb{Z}^2); \\ L_h w_h(\boldsymbol{x}^j) &= \sum_{\boldsymbol{\kappa}\in\boldsymbol{V}} s_{\boldsymbol{\kappa}} w_h(\boldsymbol{x}^j + \boldsymbol{\kappa}h), \end{aligned}$$

with constant coefficients $s_{\boldsymbol{\kappa}} \in \mathbb{R}$ (or $\mathbb{C}$), where $w_h(\boldsymbol{x}^j)$ is a function in $l^2(\mathbf{G}_h^j)$. Here, $\boldsymbol{V}$ is a finite index set. Note that since L_h is Toeplitz, it is diagonalized by the Fourier modes $\varphi(\boldsymbol{\theta}, \boldsymbol{x}^j) = e^{i\boldsymbol{\theta}\cdot\boldsymbol{x}^j/\boldsymbol{h}} = e^{i\theta_1 x_1^j/h} e^{i\theta_2 x_2^j/h}$.

Definition 2.1
If for all grid functions $\varphi(\boldsymbol{\theta}, \boldsymbol{x}^j)$,

$$L_h \varphi(\boldsymbol{\theta}, \boldsymbol{x}^j) = \widetilde{L}_h(\boldsymbol{\theta}) \varphi(\boldsymbol{\theta}, \boldsymbol{x}^j),$$

we call $\widetilde{L}_h(\boldsymbol{\theta}) = \sum_{\boldsymbol{\kappa}\in\boldsymbol{V}} s_{\boldsymbol{\kappa}} e^{i\boldsymbol{\theta}\boldsymbol{\kappa}}$ the symbol of L_h.

The staggered discretization of the Stokes equations leads to the system

$$\mathcal{L}_h \mathbf{u}_h = \begin{pmatrix} -\triangle_h & 0 & (\partial_x)_{h/2} \\ 0 & -\triangle_h & (\partial_y)_{h/2} \\ -(\partial_x)_{h/2} & -(\partial_y)_{h/2} & 0 \end{pmatrix} \begin{pmatrix} u_h \\ v_h \\ p_h \end{pmatrix}$$

with stencils

$$-\triangle_h = \frac{1}{h^2} \begin{bmatrix} & -1 & \\ -1 & 4 & -1 \\ & -1 & \end{bmatrix}, \quad (\partial_x)_h = \frac{1}{h} \begin{bmatrix} -1 & 0 & 1 \end{bmatrix}, \quad (\partial_y)_h = \frac{1}{h} \begin{bmatrix} 1 \\ 0 \\ -1 \end{bmatrix}.$$

The symbol of operator $\mathcal{L}_h$ is given by

$$\widetilde{\mathcal{L}}_h(\theta_1, \theta_2) = \frac{1}{h^2} \begin{pmatrix} 4m(\boldsymbol{\theta}) & 0 & i2h\sin\frac{\theta_1}{2} \\ 0 & 4m(\boldsymbol{\theta}) & i2h\sin\frac{\theta_2}{2} \\ -i2h\sin\frac{\theta_1}{2} & -i2h\sin\frac{\theta_2}{2} & 0 \end{pmatrix},$$

where $m(\boldsymbol{\theta}) = \frac{4-2\cos\theta_1-2\cos\theta_2}{4} = \sin^2(\frac{\theta_1}{2}) + \sin^2(\frac{\theta_2}{2})$. Each entry in $\widetilde{\mathcal{L}}_h$ is computed as the (scalar) symbol of the corresponding block of $\mathcal{L}_h$, following Definition 2.1. Since $\mathcal{L}_h$ is a 3×3

block operator, its symbol is naturally a 3×3 matrix. The error-propagation symbol for a relaxation scheme, represented by matrix M, applied to MAC scheme is

$$\widetilde{\mathcal{S}}_h(\boldsymbol{p}, \omega, \boldsymbol{\theta}) = I - \omega \widetilde{M}^{-1} \widetilde{\mathcal{L}}_h,$$

where $\boldsymbol{p}$ represents parameters within M, the block approximation to $\mathcal{L}_h$, ω is an overall weighting factor, and $\widetilde{M}$ and $\widetilde{\mathcal{L}}_h$ are the symbols for M and $\mathcal{L}_h$, respectively.

In this paper, we consider multigrid methods for staggered discretizations with standard geometric grid coarsening; that is, we construct a sequence of coarse grids by doubling the mesh size in each spatial direction. High and low frequencies for standard coarsening are given by

$$\boldsymbol{\theta} \in T^{\text{low}} = \left[-\frac{\pi}{2}, \frac{\pi}{2}\right)^2, \boldsymbol{\theta} \in T^{\text{high}} = \left[-\frac{\pi}{2}, \frac{3\pi}{2}\right)^2 \Big\backslash \left[-\frac{\pi}{2}, \frac{\pi}{2}\right)^2.$$

Definition 2.2
The error-propagation symbol, $\widetilde{\mathcal{S}}_h(\boldsymbol{\theta})$, for a block smoother $\mathcal{S}_h$ on the infinite grid $\mathbf{G}_h$ satisfies

$$\mathcal{S}_h \varphi(\boldsymbol{\theta}, \boldsymbol{x}_{k_1,k_2}) = \widetilde{\mathcal{S}}_h \varphi(\boldsymbol{\theta}, \boldsymbol{x}_{k_1,k_2}), \;\; \boldsymbol{\theta} \in \big[-\frac{\pi}{2}, \frac{3\pi}{2}\big)^2,$$

for all $\varphi(\boldsymbol{\theta}, \boldsymbol{x}_{k_1,k_2})$, and the corresponding smoothing factor for $\mathcal{S}_h$ is given by

$$\mu_{\text{loc}} = \mu_{\text{loc}}(\mathcal{S}_h) = \max_{\boldsymbol{\theta} \in T^{\text{high}}} \left\{ \left| \lambda(\widetilde{\mathcal{S}}_h(\boldsymbol{\theta})) \right| \right\},$$

where $\lambda\big(\widetilde{\mathcal{S}}_h(\boldsymbol{\theta})\big)$ is an eigenvalue of the 3×3 matrix-valued function $\widetilde{\mathcal{S}}_h(\boldsymbol{\theta})$. Throughout the rest of this paper, the developed theory applies to discrete spaces. Therefore, except when necessary for clarity, we drop the subscript h for simplicity.

Definition 2.3
Since the smoothing factor is a function of some parameters, let $\mathcal{D}$ be the set of allowable parameters and define the optimal smoothing factor over $\mathcal{D}$ as

$$\mu_{\text{opt}} = \min_{\mathcal{D}} \mu_{\text{loc}}.$$

Set $\mathcal{D}$ may have many parameters depending on the selection of the relaxation scheme.

3. DISTRIBUTIVE RELAXATION

Distributive Gauss-Seidel relaxation [6, 8] is well-known to be highly efficient for the MAC discretization. The idea of distributive relaxation is as follows. To relax the equation $\mathcal{L}x = b$, we introduce a new variable $\hat{x}$ by $x = \mathcal{P}\hat{x}$ and consider the (transformed) system $\mathcal{L}^*\hat{x} = \mathcal{L}\mathcal{P}\hat{x} = b$. Here, $\mathcal{P}$ is chosen such that the resulting operator $\mathcal{L}\mathcal{P}$ is suitable for decoupled relaxation with a simple, efficient relaxation process, preferably for each of the equations (velocity and pressure) of the transformed system separately. After each sweep of relaxation, the correction $\delta\hat{x}$, is distributed to the original unknowns, $\delta x = \mathcal{P}\delta\hat{x}$. Distributive Gauss-Seidel-type relaxation has been widely used [25, 32]. Here, we consider distributive weighted-Jacobi (DWJ) relaxation. For the Stokes equations, the discretized distribution operator can be represented by the preconditioner

$$\mathcal{P} = \begin{pmatrix} I_h & 0 & (\partial_x)_{h/2} \\ 0 & I_h & (\partial_y)_{h/2} \\ 0 & 0 & \triangle_h \end{pmatrix}.$$

Then, we apply block weighted-Jacobi relaxation to the distributed operator

$$\mathcal{L}^* = \mathcal{L}\mathcal{P} = \begin{pmatrix} -\triangle_h & 0 & 0 \\ 0 & -\triangle_h & 0 \\ -(\partial_x)_{h/2} & -(\partial_y)_{h/2} & -\triangle_h \end{pmatrix}. \qquad (4)$$

Prepared using nlaauth.cls

DOI: 10.1002/nla

Remark 3.1
For the staggered MAC discretization, if the original problem has Dirichlet boundary conditions, then the last block operator, $-\triangle_h$, of $\mathcal{L}^*$ is the standard 5-point stencil of the Laplacian operator discretized at cell centers with Neumann boundary conditions [33]. If the original problem has periodic boundary conditions, then last block operator, $-\triangle_h$, should have periodic boundary conditions.

The discrete matrix form of $\mathcal{P}$ is

$$\mathcal{P} = \begin{pmatrix} I & B^T \\ 0 & -A_p \end{pmatrix},$$

where A_p is the the standard 5-point stencil of the Laplacian operator discretized at cell centers (see Remark 3.1). For distributive weighted-Jacobi (with weight α_D) relaxation, we need to solve a system of the form

$$M\delta\hat{x} = \begin{pmatrix} \alpha_D \mathrm{diag}(A) & 0 \\ B & \alpha_D \mathrm{diag}(A_p) \end{pmatrix} \begin{pmatrix} \delta\hat{\mathcal{U}} \\ \delta\hat{p} \end{pmatrix} = \begin{pmatrix} r_{\mathcal{U}} \\ r_p \end{pmatrix}, \tag{5}$$

then distribute the updates as $\delta x = \mathcal{P}\delta\hat{x}$. The error propagation operator for the scheme is, then, $I - \omega_D \mathcal{P}\mathcal{M}^{-1}\mathcal{L}$.

3.1. *Distributive weighted-Jacobi relaxation*

The symbol of operator $\mathcal{L}^*$ is given by

$$\widetilde{\mathcal{L}}^*(\theta_1,\theta_2) = \frac{1}{h^2}\begin{pmatrix} 4m(\boldsymbol{\theta}) & 0 & 0 \\ 0 & 4m(\boldsymbol{\theta}) & 0 \\ -i2h\sin\frac{\theta_1}{2} & -i2h\sin\frac{\theta_2}{2} & 4m(\boldsymbol{\theta}) \end{pmatrix},$$

and the symbol of the block weighted-Jacobi operator is

$$\widetilde{M}_D(\theta_1,\theta_2) = \frac{1}{h^2}\begin{pmatrix} 4\alpha_D & 0 & 0 \\ 0 & 4\alpha_D & 0 \\ -i2h\sin\frac{\theta_1}{2} & -i2h\sin\frac{\theta_2}{2} & 4\alpha_D \end{pmatrix}.$$

It is easy to see that all of the eigenvalues of the error-propagation symbol, $\widetilde{\mathcal{S}}_D(\alpha_D,\omega_D,\boldsymbol{\theta}) = I - \omega_D\widetilde{\mathcal{P}}\widetilde{M}_D^{-1}\widetilde{\mathcal{L}}$, are $1-\omega_D\frac{m(\boldsymbol{\theta})}{\alpha_D}$.

Theorem 3.1
The optimal smoothing factor for distributive weighted-Jacobi relaxation is

$$\mu_{\mathrm{opt},D} = \min_{(\alpha_D,\omega_D)}\max_{\boldsymbol{\theta}\in T^{\mathrm{high}}}\left|\lambda(\widetilde{\mathcal{S}}_D(\alpha_D,\omega_D,\boldsymbol{\theta}))\right| = \frac{3}{5},$$

and is achieved if and only if $\alpha_D = \frac{5}{4}\omega_D$.

Proof
When $\boldsymbol{\theta}\in T^{\mathrm{high}}$, $m(\boldsymbol{\theta}) = \sin^2(\frac{\theta_1}{2}) + \sin^2(\frac{\theta_2}{2})$ covers the interval $[\frac{1}{2},2]$. Since all of the eigenvalues of $\widetilde{\mathcal{S}}_D(\alpha_D,\omega_D,\boldsymbol{\theta}) = I-\omega_D\widetilde{\mathcal{P}}\widetilde{M}_D^{-1}\widetilde{\mathcal{L}}$ are $1-\omega_D\frac{m(\boldsymbol{\theta})}{\alpha_D}$, $\max_{\boldsymbol{\theta}\in T^{\mathrm{high}}}\left|\lambda(\widetilde{\mathcal{S}}_D(\alpha_D,\omega_D,\boldsymbol{\theta}))\right| = \max\left\{\left|1-\frac{\omega_D}{2\alpha_D}\right|, \left|1-\frac{2\omega_D}{\alpha_D}\right|\right\}$. In order to minimize this, setting $|1-\frac{\omega_D}{2\alpha_D}| = |1-\frac{2\omega_D}{\alpha_D}|$ obtains $\frac{\omega_D}{\alpha_D} = \frac{4}{5}$ and $|1-\frac{\omega_D}{2\alpha_D}| = \frac{3}{5}$. $\square$

Remark 3.2
The optimal smoothing factor for the ω-(damped) Jacobi relaxation for 5-point finite-difference discretization of the Laplacian is $\frac{3}{5}$ with $\omega = \frac{4}{5}$. Thus, it is not surprising this serves as an intuitive lower bounded on the possible performance of block relaxation schemes that include this as a piece of the overall relaxation.

DOI: 10.1002/nla

4. BRAESS-SARAZIN-TYPE RELAXATION SCHEMES

Although the distributive weighted Jacobi-type relaxation is efficient, proper construction of the preconditioner $\mathcal{P}$, is not always possible or straightforward, especially for other types of saddle-point problems. Considering this obstacle, we also analyse other block-structured relaxation schemes. Braess-Sarazin-type algorithms were originally developed as a relaxation scheme for the Stokes equations [10], requiring the solution of a greatly simplified but global saddle-point system. As a relaxation scheme for the system in (3), one solves a system of the form

$$Mx = \begin{pmatrix} \alpha C & B^T \\ B & 0 \end{pmatrix} \begin{pmatrix} \delta \mathcal{U} \\ \delta p \end{pmatrix} = \begin{pmatrix} r_{\mathcal{U}} \\ r_p \end{pmatrix}, \tag{6}$$

where C is an approximation of A, the inverse of which is easy to apply, for example I, or $\mathrm{diag}(A)$, and $\alpha > 0$ is a chosen relaxation parameter. Solutions of (6) are computed in two stages as

$$\begin{aligned} (BC^{-1}B^T)\delta p &= BC^{-1}r_{\mathcal{U}} - \alpha r_p, \\ \delta \mathcal{U} &= \frac{1}{\alpha}C^{-1}(r_{\mathcal{U}} - B^T\delta p). \end{aligned} \tag{7}$$

In practice, (7) is not solved exactly; an approximate solve is sufficient [27], such as using a simple sweep of a Gauss-Seidel or weighted Jacobi iteration. In the following, we consider two ways to solve (7): exact and inexact methods.

4.1. *Exact Braess-Sarazin relaxation*

We first take $C = \mathrm{diag}(A)$ and analyze exact Braess-Sarazin relaxation; that is solving (7) exactly. Denoting the corresponding M as M_E, the symbol of M_E is given by

$$\widetilde{M}_E(\theta_1, \theta_2) = \frac{1}{h^2} \begin{pmatrix} 4\alpha_E & 0 & i2h\sin\frac{\theta_1}{2} \\ 0 & 4\alpha_E & i2h\sin\frac{\theta_2}{2} \\ -i2h\sin\frac{\theta_1}{2} & -i2h\sin\frac{\theta_2}{2} & 0 \end{pmatrix}.$$

The symbol of the error-propagation matrix for weighted exact BSR is $\widetilde{\mathcal{S}}_E(\alpha_E, \omega_E, \boldsymbol{\theta}) = I - \omega_E \widetilde{M}_E^{-1}\widetilde{\mathcal{L}}$. A standard calculation shows that the determinant of $\widetilde{L} - \lambda \widetilde{M}_E$ is

$$\pi_E(\lambda; \alpha_E) = \frac{16 m(\boldsymbol{\theta})\alpha_E}{h^4}(\lambda - 1)^2(\lambda - \frac{m(\boldsymbol{\theta})}{\alpha_E}),$$

thus, the eigenvalues of $\widetilde{M}_E^{-1}\widetilde{\mathcal{L}}$ are $1, 1, \dfrac{m(\boldsymbol{\theta})}{\alpha_E}$.

Remark 4.1
Note that 1 is an eigenvalue of $\widetilde{M}_E^{-1}\widetilde{\mathcal{L}}$ with multiplicity 2. This result matches with the general results for constraint preconditioners in [34], which considers the distribution of eigenvalues of the left preconditioned linear system, $G^{-1}Hx = G^{-1}b$.

Theorem 4.1
The optimal smoothing factor for (weighted) exact Braess-Sarazin relaxation is

$$\mu_{\mathrm{opt},E} = \min_{(\alpha_E, \omega_E)} \max_{\boldsymbol{\theta} \in T^{\mathrm{high}}} \left| \lambda(\widetilde{\mathcal{S}}_E(\alpha_E, \omega_E, \boldsymbol{\theta})) \right| = \frac{3}{5},$$

and is achieved if and only if $\alpha_E = \frac{5}{4}\omega_E$, with $\omega_E \in [\frac{2}{5}, \frac{8}{5}]$.

Proof
Since the symbol of the error-propagation operator, $\widetilde{\mathcal{S}}_E(\alpha_E, \omega_E, \boldsymbol{\theta}) = I - \omega_E \widetilde{M}_E^{-1}\widetilde{\mathcal{L}}$, has eigenvalues $1 - \omega_E, 1 - \omega_E, 1 - \omega_E \frac{m(\boldsymbol{\theta})}{\alpha_E}$, the smoothing factor is given by $\max_{\boldsymbol{\theta} \in T^{\mathrm{high}}} \left| \lambda(\widetilde{\mathcal{S}}_E(\alpha_E, \omega_E, \boldsymbol{\theta})) \right| =$

DOI: 10.1002/nla

$\max\Big\{\big|1-\frac{\omega_E}{2\alpha_E}\big|, \big|1-\frac{2\omega_E}{\alpha_E}\big|, \big|1-\omega_E\big|\Big\}$. As in Theorem 3.1, we know that $\min_{(\alpha_E,\omega_E)}\max_{\boldsymbol{\theta}\in T^{\text{high}}}\Big\{\big|1-\frac{\omega_E}{2\alpha_E}\big|, \big|1-\frac{2\omega_E}{\alpha_E}\big|\Big\} = \frac{3}{5}$. Since $|1-\omega_E|$ should be no larger than $\frac{3}{5}$ to achieve the overall bound, we have $\omega_E\in[\frac{2}{5},\frac{8}{5}]$. □

The natural choice is to take $\omega_E = 1$, with $\alpha_E = \frac{5}{4}\omega_E = \frac{5}{4}$. In this setting, the predicted rate of multigrid convergence is very fast, again matching the smoothing performance of weighted Jacobi on the finite-difference Poisson operator. Also note that for the analysis above, we considered $C = \text{diag}(A)$ rather than $C = I$; however, the same conclusion holds for the latter case since $\text{diag}(A) = 4I$ on the infinite grid. Taking $C = I$, we obtain the same smoothing factor $\mu_{\text{opt},E}(\boldsymbol{\theta}) = \frac{3}{5}$ with $\omega_E\in[\frac{2}{5},\frac{8}{5}]$ and $\alpha_E = 5\omega_E$.

4.2. *Inexact Braess-Sarazin relaxation*

The (exact) Braess-Sarazin approach was first introduced in [10], where it was shown that a multigrid convergence rate of $O(k^{-1})$ can be achieved, where k denotes the number of smoothing steps on each level. However, there is a significant difficulty in practical use of this method because it requires an exact inversion of the Schur complement, which is very expensive. A broader class of iterative methods for Stokes problem is discussed in [27], which demonstrated that the same $O(k^{-1})$ performance can be achieved as the exact Braess-Sarazin relaxation when the pressure correction equation is not solved exactly. In [27], this inexact BSR is seen to be slightly worse than exact BSR for a finite-element discretization of the Stokes Equations, even with a strong iteration used on the Schur complement system. This motivates us to explore inexact Braess-Sarazin relaxation for the MAC discretization, wondering whether it is possible to achieve the same smoothing factor of $\frac{3}{5}$. This will be answered in the following.

Considering parallel and GPU computation, we focus on using a single sweep of weighted Jacobi iteration (with weight ω_J) to approximate the solution of Equation (7). In order to distinguish between the parameters α_E,ω_E used in the exact case, we use α_I,ω_I in the inexact case. Denote the resulting approximation matrix, M, as M_I. Considering the block factorization of M in Equation (6), we introduce the modified Schur complement that corresponds to applying only a single weighted Jacobi sweep of relaxation on the true Schur complement, $B(\alpha_I C)^{-1}B^T$, as $-S+B(\alpha_I C)^{-1}B^T$, where $C = \text{diag}(A)$ and $S = \omega_J^{-1}\text{diag}(B(\alpha_I C)^{-1}B^T)$. The stencil of $\alpha_I C$ is

$$\frac{1}{h^2}\begin{bmatrix} 4\alpha_I & 0 \\ 0 & 4\alpha_I \end{bmatrix},$$

and the stencils of $B(\alpha_I C)^{-1}B^T$ and the modified Schur complement for weighted Jacobi iteration are, respectively,

$$\frac{1}{\alpha_I}\begin{bmatrix} & -\frac{1}{4} & \\ -\frac{1}{4} & 1 & -\frac{1}{4} \\ & -\frac{1}{4} & \end{bmatrix}, \quad \frac{1}{\alpha_I}\begin{bmatrix} & -\frac{1}{4} & \\ -\frac{1}{4} & 1-\omega_J^{-1} & -\frac{1}{4} \\ & -\frac{1}{4} & \end{bmatrix}.$$

Therefore, according to the symbol formulation (2.1), the symbol of the weighted Jacobi iteration is

$$\beta = \frac{2-\cos\theta_1-\cos\theta_2-2\omega_J^{-1}}{2\alpha_I} = \frac{m(\boldsymbol{\theta})-\omega_J^{-1}}{\alpha_I}.$$

The symbol of matrix M_I is given by

$$\widetilde{M}_I(\theta_1,\theta_2) = \frac{1}{h^2}\begin{pmatrix} 4\alpha_I & 0 & i2h\sin\frac{\theta_1}{2} \\ 0 & 4\alpha_I & i2h\sin\frac{\theta_2}{2} \\ -i2h\sin\frac{\theta_1}{2} & -i2h\sin\frac{\theta_2}{2} & h^2\beta \end{pmatrix}.$$

Calculating the determinant of $\widetilde{\mathcal{L}}-\lambda\widetilde{M}_I$, we obtain the characteristic polynomial

$$\pi_I(\lambda;\alpha_I,\omega_J) = \frac{16\alpha_I(m(\boldsymbol{\theta})-\alpha_I\beta)}{h^4}\big(\lambda-\frac{m(\boldsymbol{\theta})}{\alpha_I}\big)\big(\lambda^2+\frac{\beta m(\boldsymbol{\theta})-2m(\boldsymbol{\theta})}{m(\boldsymbol{\theta})-\alpha_I\beta}\lambda+\frac{m(\boldsymbol{\theta})}{m(\boldsymbol{\theta})-\alpha_I\beta}\big) \quad (8)$$

DOI: 10.1002/nla

Note that setting $\beta = 0$ (which would require $m(\boldsymbol{\theta})\omega_J = 1$) yields $\pi_I(\lambda;\alpha_I,\omega_J) = \pi_E(\lambda;\alpha_I)$, recovering the case of exact Braess-Sarazin. In the general case (when ω_J is a constant factor), we still recognize that $\lambda_* := \frac{m(\boldsymbol{\theta})}{\alpha_I}$ is an eigenvalue for both the exact and inexact Braess-Sarazin relaxation. Therefore, the optimal smoothing factor $\mu_{\text{opt},I}$ for the inexact case cannot be smaller than $\frac{3}{5}$, and will only achieve that value if $\frac{\omega_I}{\alpha_I} = \frac{4}{5}$. Thus, it is reasonable to try $\frac{\omega_I}{\alpha_I} = \frac{4}{5}$ in the analysis of the inexact case.

To analyze the other eigenvalues of the inexact Braess-Sarazin relaxation, substituting $\beta = \frac{m(\boldsymbol{\theta})-\omega_J^{-1}}{\alpha_I}$ into (8), these two eigenvalues, λ_1, λ_2, are the roots of

$$g_I(\lambda;\alpha_I,\omega_J) = \lambda^2 + \left(\frac{m(\boldsymbol{\theta})}{\alpha_I}\big(m(\boldsymbol{\theta})\omega_J - 1\big) - 2m(\boldsymbol{\theta})\omega_J\right)\lambda + m(\boldsymbol{\theta})\omega_J. \tag{9}$$

Consequently, we have

$$\lambda_1 + \lambda_2 = \frac{m(\boldsymbol{\theta})}{\alpha_I}\big(1 - m(\boldsymbol{\theta})\omega_J\big) + 2m(\boldsymbol{\theta})\omega_J, \tag{10}$$

$$\lambda_1\lambda_2 = m(\boldsymbol{\theta})\omega_J > 0. \tag{11}$$

Denote the discriminant of the quadratic function g_I as

$$\Delta_I(\alpha_I,\omega_J) = \frac{\omega_J^2}{\alpha_I^2} m(\boldsymbol{\theta})\big(m(\boldsymbol{\theta}) - m_*\big)\big(m(\boldsymbol{\theta}) - m_+\big)\big(m(\boldsymbol{\theta}) - m_-\big), \tag{12}$$

where

$$m_* = \omega_J^{-1}, \quad m_\pm = \frac{4\alpha_I + \omega_J^{-1} \pm \sqrt{(4\alpha_I + \omega_J^{-1})^2 - (4\alpha_I)^2}}{2}.$$

For $m(\boldsymbol{\theta}) \in [0,2]$, the sign of $\Delta_I(\alpha_I,\omega_J)$ is determined by the choices of α_I,ω_J. Hence, it is important to determine the relationship of m_*, m_+, m_-, for certain choices of α_I,ω_J. The next Lemma gives a useful characterization.

Lemma 4.1
If $\alpha_I = \omega_J^{-1}$, then $m_- = m_*$. If, furthermore, $\frac{1}{2} \le \alpha_I \le 2$, then

$$\Delta_I(\alpha_I,\omega_J) \le 0, \quad \forall m(\boldsymbol{\theta}) \in [0,2].$$

Proof
Since $\alpha_I = \omega_J^{-1}$, we have

$$m_- = \frac{4\alpha_I + \omega_J^{-1} - \sqrt{(4\alpha_I + \omega_J^{-1})^2 - (4\alpha_I)^2}}{2} = \alpha_I = m_*,$$

which is the first result.

If $\frac{1}{2} \le \alpha_I \le 2$, we have

$$m_+ = \frac{4\alpha_I + \omega_J^{-1} + \sqrt{(4\alpha_I + \omega_J^{-1})^2 - (4\alpha_I)^2}}{2} = 4\alpha_I \ge 2,$$

$$m_- = \alpha_I \le 2.$$

According to the discriminant in (12) and the relationship that $\alpha_I = \omega_J^{-1}$, it follows that

$$\Delta_I(\alpha_I,\omega) = \frac{m(\boldsymbol{\theta})(m(\boldsymbol{\theta}) - 4\alpha_I)(m(\boldsymbol{\theta}) - \alpha_I)^2}{\alpha_I^4} \le 0,$$

for all $m(\boldsymbol{\theta}) \in [0,2]$. $\square$

DOI: 10.1002/nla

Theorem 4.2
If $\Delta_I(\alpha_I, \omega_J) \leq 0$, then necessary and sufficient conditions for the convergence of inexact Braess-Sarazin iteration, $\widetilde{\mathcal{S}}_I(\boldsymbol{\theta}) = I - \omega_I(\widetilde{M}_I)^{-1}\widetilde{\mathcal{L}}$, for all frequencies $\boldsymbol{\theta} \neq 0$ are

$$\begin{aligned} |1-\omega_I\lambda_*| &< 1, \quad (13)\\ (1-\omega_I\lambda_1)(1-\omega_I\lambda_2) &< 1. \quad (14) \end{aligned}$$

Proof
If $\Delta_I(\alpha_I, \omega_J) \leq 0$, then $\lambda_1 = \overline{\lambda_2}$ and $|1-\omega_I\lambda_1|^2 = |1-\omega_I\lambda_2|^2 = (1-\omega_I\lambda_1)(1-\omega_I\lambda_2)$. Thus, the necessary and sufficient condition for convergence is $(1-\omega_I\lambda_1)(1-\omega_I\lambda_2) < 1$, along with $|1-\omega_I\lambda_*| < 1$. □

Next, under the condition $\alpha_I = \omega_J^{-1}$, we optimize the smoothing factor $\mu_{\text{loc},I}(\boldsymbol{\theta})$. Considering the convergence conditions, using (10) and (11), (14) can be simplified as

$$m(\boldsymbol{\theta}) < \omega_J^{-1} + \alpha_I(2-\omega_I),$$

which should hold for all $m(\boldsymbol{\theta}) \in [0,2]$. This is clearly satisfied for all $m(\boldsymbol{\theta})$ if it is true for $m(\boldsymbol{\theta}) = 2$. From (13), since $\lambda_* = \frac{m(\boldsymbol{\theta})}{\alpha_I}$, we obtain $\omega_I < \alpha_I$. We thus define a set $\mathcal{D}^*$, of parameters that satisfy Theorem 4.2 (allowing for non-convergence when $\boldsymbol{\theta} = 0$), as well as the assumption that $\alpha_I = \frac{5}{4}\omega_I$ needed to achieve the smoothing factor of $\frac{3}{5}$, as

$$\mathcal{D}^* = \left\{ \Big(\alpha_I, \omega_J, \omega_I\Big) : \frac{1}{2} \leq \alpha_I = \omega_J^{-1} \leq 2, 2 < \alpha_I(3-\omega_I), \alpha_I = \frac{5}{4}\omega_I \right\}.$$

The next theorem demonstrates that inexact Braess-Sarazin relaxation can achieve the optimal smoothing factor of $\frac{3}{5}$.

Theorem 4.3
For $(\alpha_I, \omega_J, \omega_I) \in \mathcal{D}^*$, the optimal smoothing factor for the inexact Braess-Sarazin relaxation is

$$\mu_{\text{opt},I} = \min_{(\alpha_I,\omega_J,\omega_I)\in\mathcal{D}^*} \max_{\boldsymbol{\theta}\in T^{\text{high}}} \left\{ |1-\omega_I\lambda_*|,\ |1-\omega_I\lambda_1|,\ |1-\omega_I\lambda_2| \right\} = \frac{3}{5},$$

and is achieved if and only if $\alpha_I = \frac{5}{4}, \omega_I = 1$, and $\omega_J = \frac{4}{5}$.

Proof
Since $(\alpha_I, \omega_J, \omega_I) \in \mathcal{D}^*$, the convergence conditions are satisfied. For the high frequencies, the eigenvalues are either complex numbers or two equal real numbers, so we consider μ_{opt}^2 in place of μ_{opt}. Let us set

$$\eta^2(m(\boldsymbol{\theta})) := (1-\omega_I\lambda_1)(1-\omega_I\lambda_2).$$

Following (10) and (11), and substituting $\omega_J^{-1} = \alpha_I, \omega_I = \frac{4}{5}\alpha_I$ into $\eta^2(m(\boldsymbol{\theta}))$, we have

$$\eta^2(m(\boldsymbol{\theta})) = \frac{4}{5\alpha_I}m(\boldsymbol{\theta})^2 + (\frac{16\alpha_I}{25} - \frac{12}{5})m(\boldsymbol{\theta}) + 1.$$

Treating η^2 as a quadratic function of m, the symmetry axis is $m_0 = \dfrac{15\alpha_I - 4\alpha_I^2}{10}$. For $\alpha_I \in [\frac{1}{2}, 2]$, $m_0 \in \left[\frac{13}{20}, \frac{45}{32}\right] \subseteq \left[\frac{1}{2}, 2\right]$, achieving its maximum value at $\alpha_I = \frac{15}{8}$. This tells us that $\eta^2(m(\boldsymbol{\theta}))$ obtains its maximum at either $m(\boldsymbol{\theta}) = \frac{1}{2}$ or $m(\boldsymbol{\theta}) = 2$, so our discussion is divided into two cases. Note also that $m_0 = \frac{5}{4}$, when $\alpha_I = \frac{5}{4}$.

Case 1: If $m_0 \geq \frac{5}{4}$, then

$$\max_{\boldsymbol{\theta}\in T^{\text{high}}} \eta^2(m(\boldsymbol{\theta})) = \eta^2(m(\boldsymbol{\theta}) = \frac{1}{2}) = \frac{1}{5\alpha_I} + \frac{8\alpha_I}{25} - \frac{1}{5}.$$

DOI: 10.1002/nla

From $m_0 \geq \frac{5}{4}$ and $\alpha_I \in [\frac{1}{2}, 2]$, we have $\alpha_I \in \left[\frac{5}{4}, 2\right]$. The optimal smoothing factor is, then

$$\min_{(\alpha_I,\omega_J,\omega_I)\in\mathcal{D}^*} \max_{\boldsymbol{\theta}\in T^{\text{high}}} \eta^2(m(\boldsymbol{\theta})) = \min_{\alpha_I\in[\frac{5}{4},2]} \left\{ \frac{1}{5\alpha_I} + \frac{8\alpha_I}{25} - \frac{1}{5} \right\} = \frac{9}{25}, \tag{15}$$

where $\alpha_I = \frac{5}{4}$ obtains the minimum.

Case 2: If $m_0 \leq \frac{5}{4}$, then

$$\max_{\boldsymbol{\theta}\in T^{\text{high}}} \eta^2(m(\boldsymbol{\theta})) = \eta^2(m(\boldsymbol{\theta}) = 2) = \frac{16}{5\alpha_I} + \frac{32\alpha_I}{25} - \frac{19}{5}.$$

From $m_0 \leq \frac{5}{4}$ and $\alpha_I \in \left[\frac{1}{2}, 2\right]$, we have $\alpha_I \in \left[\frac{1}{2}, \frac{5}{4}\right]$. The optimal smoothing factor is

$$\min_{(\alpha_I,\omega_J,\omega_I)\in\mathcal{D}^*} \max_{\boldsymbol{\theta}\in T^{\text{high}}} \eta^2(m(\boldsymbol{\theta})) = \min_{\alpha_I\in[\frac{1}{2},\frac{5}{4}]} \left\{ \frac{16}{5\alpha_I} + \frac{32\alpha_I}{25} - \frac{19}{5} \right\} = \frac{9}{25}, \tag{16}$$

where $\alpha_I = \frac{5}{4}$ obtains the minimum.

For both situations, $\omega_I = \frac{4}{5}\alpha_I = 1, \omega_J = \alpha_I^{-1} = \frac{4}{5}$ satisfy the condition $2 < \alpha_I(3 - \omega_I)$ in $\mathcal{D}^*$. Combining (15) and (16), we see that the optimal smoothing factor over $\mathcal{D}^*$ for λ_1, λ_2 is $\frac{3}{5}$. For the third eigenvalue, λ_*, since $\alpha_I = \frac{5}{4}\omega_I$ is a condition on $\mathcal{D}^*$, we always have $\max_{\boldsymbol{\theta}\in T^{\text{high}}} \left|1 - \omega_I \frac{m(\boldsymbol{\theta})}{\alpha_I}\right| = \frac{3}{5}$ as in the exact Braess-Sarazin relaxation. Thus, we can draw the conclusion that the optimal smoothing factor for inexact Brazess-Sarazin relaxation is

$$\min_{(\alpha_I,\omega_J,\omega_I)\in\mathcal{D}^*} \max_{\boldsymbol{\theta}\in T^{\text{high}}} \left\{ |1 - \omega_I\lambda_*|,\, |1 - \omega_I\lambda_1|,\, |1 - \omega_I\lambda_2| \right\} = \frac{3}{5},$$

with $\alpha_I = \frac{5}{4}, \omega_I = 1$, and $\omega_J = \frac{4}{5}$. □

Remark 4.2
For the optimal values $\alpha_I = \omega_J^{-1} = \frac{5}{4}$, and $\omega_I = 1$, (9) has real roots only for $m(\boldsymbol{\theta}) = 0, \frac{5}{4}$. For other $m(\boldsymbol{\theta}) \in [0, 2]$, the roots are complex.

Remark 4.3
It is interesting that the optimal parameter of $\alpha_I = \frac{5}{4}$ matches that found experimentally in [35] for solving the discretized Stokes problem using Taylor-Hood elements with Braess-Sarazin relaxation.

Remark 4.4
The definition of $\mathcal{D}^*$ makes use of the assumption that $\alpha_I = \omega_J^{-1}$, which is not strictly necessary, Thus, while the choice of parameters is unique over $\mathcal{D}^*$, it may not be globally unique. However, since our interest is whether IBSR can reach the same optimal smoothing factor as BSR, we do not consider this question further.

Comparing Theorem 4.3 with Theorem 4.1, we note that inexact and exact Braess-Sarazin relaxation obtain the same optimal smoothing factor, $\frac{3}{5}$, with the same choices $\alpha_I = \frac{5}{4}, \omega_I = 1$. The inexact Braess-Sarazin relaxation is simple to implement, avoiding the necessity of computing the exact inversion of the Schur complement. These properties make inexact Braess-Sarazin relaxation attractive as a smoother for general saddle-point problems.

5. UZAWA-TYPE RELAXATION

Multigrid methods with Uzawa-type relaxation are a popular family of algorithms for solving saddle-point systems [11, 36]. Each step of the exact Uzawa algorithm requires the solution of a linear system with coefficient matrix A, as well as one with an approximation of the Schur complement, $-BA^{-1}B^T$. However, if this computation is replaced by approximate solutions produced by iterative methods then, with relatively modest requirements on the accuracy of the approximate solution, the resulting inexact Uzawa algorithm is convergent, with a convergence rate close to that of the exact algorithm [36, 37]. In order to distinguish the parameters from those used in Braess-Sarazin relaxation, we add the subscript U in the following. The Uzawa-type relaxation that we consider can be written as a simpler block solve than that used in BSR,

$$M_U \delta x = \begin{pmatrix} \alpha C & 0 \\ B & -S \end{pmatrix} \begin{pmatrix} \delta \mathcal{U} \\ \delta p \end{pmatrix} = \begin{pmatrix} r_{\mathcal{U}} \\ r_p \end{pmatrix}, \tag{17}$$

where αC is an approximation of A and $-S$ is an approximation of the Schur complement, $-BA^{-1}B^T$.

Here, we discuss two cases. First, we consider an analogue to exact Braess-Sarazin with $C = \mathrm{diag}(A), S = B(\alpha C)^{-1}B^T$. Then, we consider an algorithm with manageable cost, with $C = \mathrm{diag}(A), S = \sigma^{-1}I$.

5.1. *Schur-Uzawa relaxation*

Here, we consider $C = \mathrm{diag}(A)$, $S = B(\alpha_{SU}C)^{-1}B^T$, giving the so-called Schur-Uzawa method. The amplification factor for this method is $\widetilde{\mathcal{S}}_{SU}(\alpha_{SU}, \omega_{SU}, \boldsymbol{\theta}) = I - \omega_{SU}\widetilde{M}_{SU}^{-1}\widetilde{\mathcal{L}}$ and the symbol of M_{SU} is given by

$$\widetilde{M}_{SU}(\theta_1, \theta_2) = \frac{1}{h^2} \begin{pmatrix} 4\alpha_{SU} & 0 & 0 \\ 0 & 4\alpha_{SU} & 0 \\ -i2h\sin\frac{\theta_1}{2} & -i2h\sin\frac{\theta_2}{2} & -\frac{m(\boldsymbol{\theta})}{\alpha_{SU}}h^2 \end{pmatrix}.$$

The determinant of $\widetilde{L} - \lambda\widetilde{M}_{SU}$ is then

$$\pi_{SU}(\lambda; \alpha_{SU}) = \frac{16\alpha_{SU}m(\boldsymbol{\theta})}{h^4}\big(\lambda - \frac{m(\boldsymbol{\theta})}{\alpha_{SU}}\big)\Big(\lambda^2 - \big(1 + \frac{m(\boldsymbol{\theta})}{\alpha_{SU}}\big)\lambda + 1\Big).$$

As discussed in Braess-Sarazin relaxation, the optimal smoothing factor for the modes $\lambda_{*_U} := \frac{m(\boldsymbol{\theta})}{\alpha_{SU}}$ is known to be

$$\big|1 - \frac{2\omega_{SU}}{\alpha_{SU}}\big| = \big|1 - \frac{\omega_{SU}}{2\alpha_{SU}}\big| = \frac{3}{5},$$

provided that $\frac{\omega_{SU}}{\alpha_{SU}} = \frac{4}{5}$.

To analyze the other eigenvalues of Schur-Uzawa relaxation, we denote λ_1, λ_2 as the roots of

$$g_{SU}(\lambda; \alpha_{SU}) = \lambda^2 - \big(1 + \frac{m(\boldsymbol{\theta})}{\alpha_{SU}}\big)\lambda + 1, \tag{18}$$

taking the discriminant of the quadratic function g_{SU} as

$$\Delta_{SU}(m(\boldsymbol{\theta}); \alpha_{SU}) = \big(1 + \frac{m(\boldsymbol{\theta})}{\alpha_{SU}}\big)^2 - 4.$$

Since the sign of the discriminant is undetermined and depends on the value of $m(\boldsymbol{\theta})$, we must consider three cases for the distribution of the eigenvalues. First, that all of the eigenvalues are real numbers. Second, that all of the eigenvalues are complex numbers. Finally, that some are real and some are complex. The main idea behind optimizing the smoothing factor is, simply, to optimize for each of the three cases respectively, then select the best one.

Theorem 5.1
The optimal smoothing factor for Schur-Uzawa relaxation is

$$\begin{aligned} \mu_{\mathrm{opt},SU} &= \min_{(\alpha_{SU},\omega_{SU})} \max_{\boldsymbol{\theta}\in T^{\mathrm{high}}} \Big\{ \big|\lambda(\widetilde{\mathcal{S}}_{SU}(\alpha_{SU}, \omega_{SU}, \boldsymbol{\theta}))\big| \Big\} \\ &= \sqrt{\frac{33 - 3\sqrt{73}}{41 - 3\sqrt{73}}} \approx 0.6924, \end{aligned}$$

DOI: 10.1002/nla

and is achieved if and only if

$$\alpha_{SU} = \frac{4}{\sqrt{73}-5}, \, \omega_{SU} = \frac{4}{\sqrt{73}-3}.$$

Proof

Case 1: If $\Delta_{SU}(m(\boldsymbol{\theta});\alpha_{SU}) \leq 0$ for all $m(\boldsymbol{\theta})$, then we must have $\alpha_{SU} \geq m(\boldsymbol{\theta})$ for all $\boldsymbol{\theta}$, so $\alpha_{SU} \geq 2$. In this case, we have two complex roots for all $m(\boldsymbol{\theta})$, whose magnitude, $\tau_{SU}(m(\boldsymbol{\theta}))$, is given by

$$\begin{aligned} \tau^2_{SU}(m(\boldsymbol{\theta})) &:= (1-\omega_{SU}\lambda_1)(1-\omega_{SU}\lambda_2), \\ &= 1-(\lambda_1+\lambda_2)\omega_{SU}+\lambda_1\lambda_2\omega^2_{SU}, \\ &= 1-\omega_{SU}(1+\frac{m(\boldsymbol{\theta})}{\alpha_{SU}})+\omega^2_{SU}. \end{aligned}$$

The smoothing factor over these roots is given by

$$\begin{aligned} \mu_C(\alpha_{SU},\omega_{SU})^2 : &= \max_{m(\boldsymbol{\theta})\in[\frac{1}{2},2]} \tau^2_{SU}(m(\boldsymbol{\theta})) = \tau^2_{SU}(\frac{1}{2}) \\ &= \left(\omega_{SU} - (\frac{1}{2}+\frac{1}{4\alpha_{SU}})\right)^2 + 1 - (\frac{1}{2}+\frac{1}{4\alpha_{SU}})^2. \end{aligned} \tag{19}$$

In order to minimize $\mu_C(\alpha_{SU},\omega_{SU})$, ω_{SU} must be equal to $\omega^*_{SU} = \frac{1}{2}+\frac{1}{4\alpha_{SU}}$. Since $\alpha_{SU}\geq 2$,

$$\min_{(\alpha_{SU}\geq 2,\omega_{SU})} \mu_C = \sqrt{1-(\frac{1}{2}+\frac{1}{4\times 2})^2} = \sqrt{\frac{39}{64}} \approx 0.7806,$$

provided that $\alpha_{SU}=2, \omega_{SU}=\frac{1}{2}+\frac{1}{4\alpha_{SU}}=\frac{5}{8}$.

Since there is another eigenvalue, $\frac{m(\boldsymbol{\theta})}{\alpha_{SU}}$, the optimal smoothing factor when $\Delta_{SU}(m(\boldsymbol{\theta});\alpha_{SU}) \leq 0$ for all $\boldsymbol{\theta}$ is at least $\sqrt{\frac{39}{64}}$.

Case 2: If $\Delta_{SU}(m(\boldsymbol{\theta});\alpha_{SU}) \geq 0$ for all $m(\boldsymbol{\theta})$, then we have $\alpha_{SU}\leq m(\boldsymbol{\theta})$ for all $\boldsymbol{\theta}$, so $\alpha_{SU}\leq\frac{1}{2}$. Denote the two eigenvalues of (18) as $\lambda_+(m(\boldsymbol{\theta})) > \lambda_-(m(\boldsymbol{\theta}))$. It is easy to check that λ_+ is an increasing function of $m(\boldsymbol{\theta})$, while λ_- is a decreasing function of $m(\boldsymbol{\theta})$. Set

$$\mu_R(\alpha_{SU},\omega_{IU}) := \max_{m(\boldsymbol{\theta})\in[\frac{1}{2},2]} \{|1-\omega_{SU}\lambda|\} = \max\left\{|1-\omega_{SU}\lambda_+(2)|, |1-\omega_{SU}\lambda_-(2)|\right\}. \tag{20}$$

We know that to minimize this maximum, we need

$$\omega_{SU} = \frac{2}{\lambda_+(2)+\lambda_-(2)} = \frac{2}{\frac{2}{\alpha_{SU}}+1}, \tag{21}$$

and take $\omega^{**}_{SU} = \frac{2}{\frac{2}{\alpha_{SU}}+1}$. The smoothing factor for these modes is then given by

$$\begin{aligned} \min\mu_R(\alpha_{SU},\omega_{SU}) &= \min_{\alpha_{SU}\leq\frac{1}{2}} \left\{\frac{\lambda_+(2)-\lambda_-(2)}{\lambda_+(2)+\lambda_-(2)}\right\} \\ &= \min_{\alpha_{SU}\leq\frac{1}{2}} \left\{\sqrt{1-\frac{4\lambda_+(2)\lambda_-(2)}{\left(\lambda_+(2)+\lambda_-(2)\right)^2}}\right\} \\ &= \min_{\alpha_{SU}\leq\frac{1}{2}} \left\{\sqrt{1-\omega^2_{SU}}\right\} \\ &= \sqrt{\frac{21}{25}} \approx 0.9615, \end{aligned} \tag{22}$$

DOI: 10.1002/nla

since $\lambda_+(2)\lambda_-(2) = 1$ with the minimum achieved when $\alpha_{SU} = \frac{1}{2}$.

Since there is another eigenvalue, $\frac{m(\boldsymbol{\theta})}{\alpha_{SU}}$, the optimal smoothing factor when $\Delta_{SU}(m(\boldsymbol{\theta});\alpha_{SU}) \geq 0$ for all $\boldsymbol{\theta}$ is at least $\sqrt{\frac{21}{25}}$.

Case 3: $\alpha_{SU} \in (\frac{1}{2}, 2)$. When $m(\boldsymbol{\theta}) \in (\frac{1}{2}, \alpha_{SU}]$, $\Delta_{SU}(m(\boldsymbol{\theta});\alpha_{SU}) \leq 0$. From (19), we know that $\mu_C(\alpha_{SU}, \omega_{SU})$ is an increasing function of α_{SU}. When $m(\boldsymbol{\theta}) \in [\alpha_{SU}, 2)$, $\Delta_{SU}(m(\boldsymbol{\theta});\alpha_{SU}) \geq 0$. From (21) and (22), we know that $\mu_R(\alpha_{SU}, \omega_{SU})$ is a decreasing function of α_{SU}. Set

$$\mu_{SU} = \min_{(\alpha_{SU}, \omega_{SU})} \max\Big\{ \max_{\alpha_{SU} \leq \boldsymbol{\theta} < 2} \mu_R(\alpha_{SU}, \omega_{SU}), \max_{\frac{1}{2} \leq \boldsymbol{\theta} \leq \alpha_{SU}} \mu_C(\alpha_{SU}, \omega_{SU}) \Big\}.$$

In order to achieve the minimum, we must have $\mu_R(\alpha_{SU}, \omega_{SU}) = \mu_C(\alpha_{SU}, \omega_{SU})$ and $\omega^*_{SU} = \omega^{**}_{SU}$. This gives $\alpha_{SU} = \frac{4}{\sqrt{73}-5}$, $\omega_{SU} = \frac{4}{\sqrt{73}-3}$, and

$$\mu_{SU} = \sqrt{1 - \omega^2_{SU}} = \sqrt{\frac{33 - 3\sqrt{73}}{41 - 3\sqrt{73}}} \approx 0.6924.$$

Recall the third eigenvalue $\frac{m(\boldsymbol{\theta})}{\alpha_{SU}}$. Since $\alpha_{SU} = \frac{4}{\sqrt{73}-5}$ and $\omega_{SU} = \frac{4}{\sqrt{73}-3}$, we have

$$\max_{m(\boldsymbol{\theta}) \in [\frac{1}{2}, 2]} \left\{ \left|1 - \omega_{SU} \frac{m(\boldsymbol{\theta})}{\alpha_{SU}}\right| \right\} = \frac{70 + 2\sqrt{73}}{128} \approx 0.6804 < 0.6924.$$

From the three cases discussed above, we can clearly conclude that when $\alpha_{SU} = \frac{4}{\sqrt{73}-5}$ and $\omega_{SU} = \frac{4}{\sqrt{73}-3}$, we obtain the optimal smoothing factor $\mu_{SU} = \sqrt{\frac{33-3\sqrt{73}}{41-3\sqrt{73}}} \approx 0.6924$. $\square$

We note that the convergence factor predicated for Schur-Uzawa is somewhat worse than for exact Braess-Sarazin. As we will see in the next section, further degradation occurs when we consider the more practical algorithm, σ-Uzawa.

5.2. *σ-Uzawa relaxation*

In Braess-Sarazin relaxation, we prefer to solve Schur complement system $(BC^{-1}B^T)\delta p = BC^{-1}r_{\mathcal{U}} - \alpha r_p$ by an inexact iteration such as weighted Jacobi for the pressure update. This idea can be adopted to the Schur-Uzawa relaxation, replacing the exact solution of $B(\alpha_{SU}C)^{-1}B^T\delta p = B\delta\mathcal{U} - r_p$ by the simple calculation of $\sigma^{-1}\delta p = B\delta\mathcal{U} - r_p$, which can be viewed as a weighted Jacobi iteration applied with the Schur-Uzawa solve, since the symbol of $\mathrm{diag}(B(\alpha_{SU}C)^{-1}B^T)$ is α_{SU}^{-1}. Following the usual notation, we call the resulting parameter σ and the algorithm as σ-Uzawa relaxation. The symbol of the resulting approximation of $\mathcal{L}$, M_U, is given by

$$\widetilde{M_U}(\theta_1, \theta_2) = \frac{1}{h^2}\begin{pmatrix} 4\alpha_U & 0 & 0 \\ 0 & 4\alpha_U & 0 \\ -i2h\sin\frac{\theta_1}{2} & -i2h\sin\frac{\theta_2}{2} & -\sigma^{-1}h^2 \end{pmatrix}.$$

The determinant of $\widetilde{L} - \lambda\widetilde{M_U}$ is then

$$\pi_U(\lambda; \alpha_U, \sigma) = \frac{16\alpha_U^2}{\sigma h^4}\big(\lambda - \frac{m(\boldsymbol{\theta})}{\alpha_U}\big)\left(\lambda^2 - \frac{1+\sigma}{\alpha_U}m(\boldsymbol{\theta})\lambda + \frac{m(\boldsymbol{\theta})\sigma}{\alpha_U}\right).$$

Since $\lambda_{*_U} := \frac{m(\boldsymbol{\theta})}{\alpha_U}$ and $m(\boldsymbol{\theta}) \in [\frac{1}{2}, 2]$ for high frequencies, the optimal smoothing factor for these modes is known to be

$$\left|1 - \frac{2\omega_U}{\alpha_U}\right| = \left|1 - \frac{\omega_U}{2\alpha_U}\right| = \frac{3}{5},$$

provided that $\frac{\omega_U}{\alpha_U} = \frac{4}{5}$.

DOI: 10.1002/nla

To analyze the other eigenvalues of σ-Uzawa relaxation, we denote by λ_1, λ_2 the roots of

$$g_U(\lambda;\alpha_U,\sigma) = \lambda^2 - \frac{(1+\sigma)m(\boldsymbol{\theta})}{\alpha_U}\lambda + \frac{m(\boldsymbol{\theta})\sigma}{\alpha_U}, \tag{23}$$

taking the discriminant of the quadratic function g_U as

$$\Delta_U(\alpha_U,\sigma) = \frac{m(\boldsymbol{\theta})(1+\sigma)^2}{\alpha_U^2}\left(m(\boldsymbol{\theta}) - \frac{4\alpha_U\sigma}{(1+\sigma)^2}\right),$$

and take

$$m_1 = 0, \quad m_2 = \frac{4\alpha_U\sigma}{(1+\sigma)^2}.$$

From (23), we have

$$\lambda_1 + \lambda_2 = \frac{m(\boldsymbol{\theta})(1+\sigma)}{\alpha_U} > 0, \tag{24}$$

$$\lambda_1\lambda_2 = \frac{m(\boldsymbol{\theta})\sigma}{\alpha_U} > 0, \tag{25}$$

$$\lambda_{1,2} = \frac{(1+\sigma)m(\boldsymbol{\theta})}{2\alpha_U}\left(1 \pm \sqrt{1 - \frac{m_2}{m(\boldsymbol{\theta})}}\right). \tag{26}$$

The sign of $\Delta_U(\alpha_U,\sigma)$ (and, consequently, the value of m_2) plays an important role in the analysis of the smoothing factor. As before, we explore the optimal smoothing factor for three cases: only real eigenvalues, only complex eigenvalues, and when $\frac{1}{2} < m_2 < 2$, giving both real and complex eigenvalues. We first explore the case where only complex eigenvalues occur.

In order to discuss the complex eigenvalues, we take $\tau(m(\boldsymbol{\theta}))$ to be the magnitude of the two eigenvalues at frequency $\boldsymbol{\theta}$, giving

$$\begin{aligned}\tau^2(m(\boldsymbol{\theta})) &= (1-\omega_U\lambda_1)(1-\omega_U\lambda_2),\\ &= 1-(\lambda_1+\lambda_2)\omega_U + \lambda_1\lambda_2\omega_U^2,\\ &= 1+\frac{\omega_U}{\alpha_U}(\omega_U\sigma-\sigma-1)m(\boldsymbol{\theta}).\end{aligned}$$

For simplicity of discussion of the smoothing factor for complex eigenvalues, we give a general result that can be applied in the third case, when $\frac{1}{2} < m_2 < 2$.

Lemma 5.1
Assume that $m_2 \geq \frac{1}{2}$ and let $\gamma = \min\{m_2, 2\}$. For $m(\boldsymbol{\theta}) \in [\frac{1}{2}, \gamma]$, eigenvalues λ_1 and λ_2 are complex conjugates and the smoothing factor for these modes over this range of $\boldsymbol{\theta}$ is

$$SF_C = \max_{m(\boldsymbol{\theta})\in[\frac{1}{2},\gamma]} \tau(m(\boldsymbol{\theta})) = \sqrt{1+\frac{\omega_U(\omega_U\sigma-\sigma-1)}{\alpha_U}} \geq \sqrt{1-\frac{1}{2\gamma}},$$

with equality if and only if

$$\frac{\omega_U}{\alpha_U}(\omega_U\sigma-\sigma-1) = -\frac{1}{\gamma}.$$

Proof
Clearly, for $m(\boldsymbol{\theta}) \in [\frac{1}{2}, \gamma]$, $\Delta_U(\alpha_U,\sigma) \leq 0$ and $|1-\omega_U\lambda_1| = |1-\omega_U\lambda_2| = \tau(m(\boldsymbol{\theta}))$. In order to guarantee convergence, we require $\tau(m(\boldsymbol{\theta}))^2 < 1$ (with equality allowed for $\boldsymbol{\theta} = 0$). This requires that $\frac{\omega_U(\omega_U\sigma-\sigma-1)}{\alpha_U} < 0$. Since $\gamma = \min\{m_2, 2\}$, it is easily seen that

$$\begin{aligned}\tau^2(\gamma) &= 1+\frac{\omega_U}{\alpha_U}(\omega_U\sigma-\sigma-1)\gamma\\ &\geq 1+\frac{\omega_U}{\alpha_U}(\omega_U\sigma-\sigma-1)m_2\\ &= \left(1-\frac{2\omega_U\sigma}{1+\sigma}\right)^2 \geq 0,\end{aligned}$$

which gives

$$\frac{\omega_U}{\alpha_U}(\omega_U\sigma-\sigma-1)\geq -\frac{1}{\gamma}.$$

It follows that

$$\max_{m(\boldsymbol{\theta})\in[\frac{1}{2},\gamma]}\tau(m(\boldsymbol{\theta}))=\tau\left(\frac{1}{2}\right)=\sqrt{1+\frac{\omega_U}{2\alpha_U}(\omega_U\sigma-\sigma-1)}\geq\sqrt{1-\frac{1}{2\gamma}},$$

and that equality is achieved if and only if $\frac{\omega_U(\omega_U\sigma-\sigma-1)}{\alpha_U}=\frac{-1}{\gamma}$. □

Lemma 5.2
If $m_2=\frac{4\alpha_U\sigma}{(1+\sigma)^2}>2$, then $\tau^2(2)=1+\frac{\omega_U}{\alpha_U}(\omega_U\sigma-\sigma-1)2>0$.

Proof
For contradiction, assume that $\tau(2)=1+\frac{\omega_U}{\alpha_U}(\omega_U\sigma-\sigma-1)2=0$, which gives $\frac{\alpha_U}{\omega_U(\sigma+1-\omega_U\sigma)}=2$. Since $m_2>2$, we have

$$\frac{4\alpha_U\sigma}{(1+\sigma)^2}>\frac{\alpha_U}{\omega_U(\sigma+1-\omega_U\sigma)},$$

which can be rewritten as

$$\left(\frac{\omega_U\sigma}{1+\sigma}-\frac{1}{2}\right)^2<0.$$

□

These results allow us to obtain a bound on the smoothing factor when $m_2>2$.

Theorem 5.2
If $m_2=\frac{4\alpha_U\sigma}{(1+\sigma)^2}>2$, then the optimal smoothing factor for inexact Uzawa relaxation is larger than $\frac{\sqrt{3}}{2}$.

Proof
From Lemma 5.1, we know the smoothing factor for the complex modes is $SF_C=\tau(\frac{1}{2})\geq\sqrt{1-\frac{1}{2\gamma}}=\frac{\sqrt{3}}{2}$ with equality if and only if $\tau^2(2)=0$. However, from Lemma 5.2, we know when $m_2>2$, $\tau^2(2)\neq 0$. This implies that the optimal smoothing factor is larger than $\frac{\sqrt{3}}{2}$. □

We now consider the case where $m_2\leq 2$. For $m(\boldsymbol{\theta})\in[m_2,2]$, the two roots are real. From (26), we have

$$\begin{aligned}|1-\omega_U\lambda_1| &= \left|1-\frac{(1+\sigma)\omega_U}{2\alpha_U}m(\boldsymbol{\theta})\left(1+\sqrt{1-\frac{m_2}{m(\boldsymbol{\theta})}}\right)\right|,\\ |1-\omega_U\lambda_2| &= \left|1-\frac{(1+\sigma)\omega_U}{2\alpha_U}m(\boldsymbol{\theta})\left(1-\sqrt{1-\frac{m_2}{m(\boldsymbol{\theta})}}\right)\right|.\end{aligned}$$

Let

$$\begin{aligned}R_+(m(\boldsymbol{\theta})) &= \frac{m(\boldsymbol{\theta})}{2}\left(1+\sqrt{1-\frac{m_2}{m(\boldsymbol{\theta})}}\right),\\ R_-(m(\boldsymbol{\theta})) &= \frac{m(\boldsymbol{\theta})}{2}\left(1-\sqrt{1-\frac{m_2}{m(\boldsymbol{\theta})}}\right).\end{aligned}$$

Function $R_+(m(\boldsymbol{\theta}))$ is an increasing function of $m(\boldsymbol{\theta})$ for $m(\boldsymbol{\theta})\in[m_2,2]$, giving

$$\begin{aligned}R_1:=R_+(m(\boldsymbol{\theta}))_{\max} &= R_+(2)=1+\sqrt{1-\frac{m_2}{2}},\\ R_+(m(\boldsymbol{\theta}))_{\min} &= R_+(m_2)=\frac{m_2}{2}.\end{aligned}$$

For function $R_-(m(\boldsymbol{\theta}))$, since it is a decreasing function of $m(\boldsymbol{\theta})$, where $m(\boldsymbol{\theta}) \in [m_2, 2]$, we have

$$\begin{aligned} R_-(m(\boldsymbol{\theta}))_{\max} &= R_-(m_2) = \frac{m_2}{2}, \\ R_2 := R_-(m(\boldsymbol{\theta}))_{\min} &= R_-(2) = 1 - \sqrt{1 - \frac{m_2}{2}}. \end{aligned}$$

Remark 5.1
$R_-(m(\boldsymbol{\theta}))$ is a decreasing function of $m(\boldsymbol{\theta})$, because $R_-(m(\boldsymbol{\theta}))' = \frac{\sqrt{1-\frac{m_2}{m(\boldsymbol{\theta})}} + \frac{m_2}{2m(\boldsymbol{\theta})} - 1}{2\sqrt{1-\frac{m_2}{m(\boldsymbol{\theta})}}} < 0$ for all $m(\boldsymbol{\theta}) \in (m_2, 2]$.

From the above discussion, the smoothing factor for the two real eigenvalues in this case is

$$\begin{aligned} SF_R: &= \max_{\boldsymbol{\theta} \in T^{\text{high}}} \left|\lambda(\widetilde{\mathcal{S}}_U(\alpha_U, \omega_U, \sigma, \boldsymbol{\theta}))\right| \\ &= \max\left\{ \left|1 - \frac{(1+\sigma)\omega_U}{\alpha_U} R_1\right|, \left|1 - \frac{(1+\sigma)\omega_U}{\alpha_U} R_2\right| \right\}. \end{aligned}$$

We can simplify the above expression by noting that

$$SF_R = \begin{cases} \frac{(1+\sigma)\omega_U}{\alpha_U} R_1 - 1, & \text{if} \quad \frac{(1+\sigma)\omega_U}{\alpha_U} \geq 1 \\ 1 - \frac{(1+\sigma)\omega_U}{\alpha_U} R_2, & \text{if} \quad \frac{(1+\sigma)\omega_U}{\alpha_U} \leq 1 \end{cases} \tag{27}$$

This allows us to bound the smoothing factor for the case when $m_2 \leq \frac{1}{2}$.

Theorem 5.3
If $m_2 = \frac{4\alpha_U \sigma}{(1+\sigma)^2} \leq \frac{1}{2}$, then the optimal smoothing factor for inexact Uzawa relaxation is at least $\frac{\sqrt{3}}{2}$.

Proof
Since $m_2 \leq \frac{1}{2}$, the eigenvalues are all real. According to (27), the smoothing factor for $m(\boldsymbol{\theta}) \in [\frac{1}{2}, 2]$ is

$$SF_R = \begin{cases} \frac{(1+\sigma)\omega_U}{\alpha_U}(1 + \frac{\sqrt{3}}{2}) - 1, & \text{if} \quad \frac{(1+\sigma)\omega_U}{\alpha_U} \geq 1 \\ 1 - \frac{(1+\sigma)\omega_U}{\alpha_U}(1 - \frac{\sqrt{3}}{2}), & \text{if} \quad \frac{(1+\sigma)\omega_U}{\alpha_U} \leq 1 \end{cases}$$

It is easy to see that when $\frac{(1+\sigma)\omega_U}{\alpha} = 1$, SF_R reaches its minimum value of $\frac{\sqrt{3}}{2}$. Note that the conditions that $\frac{(1+\sigma)\omega_U}{\alpha} = 1$ and $m_2 \leq \frac{1}{2}$ might not be satisfied at the same time, so the optimal smoothing factor may be larger than $\frac{\sqrt{3}}{2}$. □

We now consider the case where $\frac{1}{2} \leq m_2 \leq 2$. The key parameter in the proof is $\frac{(1+\sigma)\omega_U}{\alpha_U}$, which determines which of bounds on the real eigenvalues is dominant.

Theorem 5.4
When $m_2 \in [\frac{1}{2}, 2]$, the optimal smoothing factor for σ-Uzawa relaxation is

$$\begin{aligned} \mu_{\text{opt},\sigma U} &= \min_{(\alpha_U, \omega_U, \sigma)} \max_{\boldsymbol{\theta} \in T^{\text{high}}} \left\{ \left|1 - \frac{2\omega_U}{\alpha_U}\right|, \left|1 - \frac{\omega_U}{2\alpha_U}\right|, SF_R, SF_C \right\} \\ &= \sqrt{1 - \frac{m_{\text{opt}}}{2}} = \sqrt{\frac{3}{5}} \approx 0.7746, \end{aligned}$$

DOI: 10.1002/nla

if and only if $m_2 = m_{\text{opt}} = \frac{4}{5}$, and the parameters satisfy

$$\begin{aligned}
\frac{1}{5(2\mu_{\text{opt},U}-1)} \leq \quad \omega_U \quad &\leq \frac{2}{5(1-\mu_{\text{opt},U})},\\
\alpha_U \quad &= \quad \frac{5\omega_U^2}{5\omega_U-1},\\
\sigma \quad &= \quad \frac{1}{5\omega_U-1}.
\end{aligned}$$

Proof
We first consider the case where $\frac{(1+\sigma)\omega_U}{\alpha_U} = 1$, and the two expressions in (27) coincide. In this case, $m_2 = \frac{4\alpha_U\sigma}{(1+\sigma)^2} = 4\frac{\omega_U^2\sigma}{\alpha_U}$, and, for $m(\boldsymbol{\theta}) \in [m_2, 2]$,

$$SF_R = \frac{(1+\sigma)\omega_U}{\alpha_U}R_1 - 1 = \sqrt{1-\frac{m_2}{2}} = \sqrt{1-2\frac{\omega_U^2\sigma}{\alpha_U}}.$$

For $m(\boldsymbol{\theta}) \in [\frac{1}{2}, m_2]$, from Lemma 5.1, we have

$$SF_C = \sqrt{1+\frac{\omega_U(\omega_U\sigma-\sigma-1)}{2\alpha_U}} = \sqrt{\frac{1}{2}+\frac{\omega_U^2\sigma}{2\alpha_U}}.$$

Since SF_R is a decreasing function of $\frac{\omega_U^2\sigma}{\alpha_U}$ and SF_C is an increasing function of $\frac{\omega_U^2\sigma}{\alpha_U}$, the optimal smoothing factor over the modes bounded by these factor is achieved if and only if $SF_R = SF_C$ and is given by

$$\mu_{\text{opt},\sigma U} = \min_{(\alpha_U,\omega_U,\sigma)} \max_{m(\boldsymbol{\theta})\in[\frac{1}{2},2]} \left\{ \sqrt{1-2\frac{\omega_U^2\sigma}{\alpha_U}}, \sqrt{\frac{1}{2}+\frac{\omega_U^2\sigma}{2\alpha_U}} \right\} = \sqrt{\frac{3}{5}}, \tag{28}$$

with the minimum occurring when

$$\frac{\omega_U^2\sigma}{\alpha_U} = \frac{1}{5}, \tag{29}$$

$$\frac{(1+\sigma)\omega_U}{\alpha_U} = 1. \tag{30}$$

Furthermore, $m_{\text{opt}} := m_2 = 4\frac{\omega_U^2\sigma}{\alpha_U} = \frac{4}{5}$. We now show this is the best possible bound over these two modes before returning to consider the eigenvalues $1-\omega_U\frac{m(\boldsymbol{\theta})}{\alpha_U}$.

In the following, take $x = \frac{(1+\sigma)\omega_U}{\alpha_U}$, and $y = \frac{\omega_U^2\sigma}{\alpha_U}$, then $m_2 = \frac{4\alpha_U\sigma}{(1+\sigma)^2} = \frac{4y}{x^2}$. Assume that $SF_C \leq \sqrt{\frac{3}{5}}$; that is

$$\sqrt{1+\frac{\omega_U(\omega_U\sigma-\sigma-1)}{2\alpha_U}} = \sqrt{1-\frac{x}{2}+\frac{y}{2}} \leq \sqrt{\frac{3}{5}},$$

which implies that

$$y \leq x - \frac{4}{5}. \tag{31}$$

If $x > 1$, from (27) and (31), we have

$$\begin{aligned} SF_R &= \frac{(1+\sigma)\omega_U}{\alpha_U}\left(1+\sqrt{1-\frac{m_2}{2}}\right)-1 \\ &= x+\sqrt{x^2-2y}-1 \\ &\geq x+\sqrt{x^2-2(x-\frac{4}{5})}-1 \\ &= x-1+\sqrt{(x-1)^2+\frac{3}{5}} \\ &> \sqrt{\frac{3}{5}}. \end{aligned}$$

Therefore, when $x > 1$, the optimal smoothing factor is larger than $\sqrt{\frac{3}{5}}$.

If $x < 1$, from (27) and (31), we have

$$\begin{aligned} SF_R &= 1-\frac{(1+\sigma)\omega_U}{\alpha_U}\left(1-\sqrt{1-\frac{m_2}{2}}\right) \\ &= 1-x+\sqrt{x^2-2y} \\ &\geq 1-x+\sqrt{x^2-2(x-\frac{4}{5})}-1 \\ &= 1-x+\sqrt{(x-1)^2+\frac{3}{5}} \\ &> \sqrt{\frac{3}{5}}. \end{aligned}$$

Therefore, when $x < 1$, the optimal smoothing factor is larger than $\sqrt{\frac{3}{5}}$.

Thus, over all choices of x, the optimal smoothing factor that over these modes is $\mu_{\text{opt},U} = \sqrt{\frac{3}{5}}$, achieved when $x = \frac{(1+\sigma_U)\omega_U}{\alpha_U} = 1$.

We now consider the eigenvalue $\lambda_{*,U} = \frac{m(\boldsymbol{\theta})}{\alpha_U}$. We know that $\min_{(\alpha_U,\omega_U,\sigma)} \max_{\boldsymbol{\theta}\in T^{\text{high}}} \left|1-\omega_U\frac{m(\boldsymbol{\theta})}{\alpha_U}\right| = \frac{3}{5} < \mu_{\text{opt},U} = \sqrt{\frac{3}{5}}$. In order to have this mode not be reduced more slowly than the others, we need

$$|1-\frac{2\omega_U}{\alpha_U}| \leq \mu_{\text{opt},U} \text{ and } |1-\frac{\omega_U}{2\alpha_U}| \leq \mu_{\text{opt},U},$$

which imply that

$$2(1-\mu_{\text{opt},U})\frac{1}{\omega_U} \leq \frac{1}{\alpha_U} \leq \frac{1+\mu_{\text{opt},U}}{2}\frac{1}{\omega_U}. \tag{32}$$

Simplifying (29) and (30) , we have

$$\alpha_U = \frac{5\omega_U^2}{5\omega_U-1}, \tag{33}$$

$$\sigma = \frac{1}{5\omega_U-1}. \tag{34}$$

Using (33) and (34), (32) can be simplified as

$$\frac{1}{5(2\mu_{\text{opt},U}-1)} \leq \omega_U \leq \frac{2}{5(1-\mu_{\text{opt},U})}. \tag{35}$$

DOI: 10.1002/nla

Note that the set of values defined by (33), (34), and (35) is not empty, with parameters $\omega_U = 1, \alpha_U = \frac{5}{4}, \sigma = \frac{1}{4}$ in this set.

$\square$

Corollary 5.1

The optimal smoothing factor for σ-Uzawa relaxation over all possible parameters is $\sqrt{\frac{3}{5}}$.

Comparing this to the optimal smoothing factor for both exact and inexact Braess-Sarazin, $\frac{3}{5}$, we note that Braess-Sarazin relaxation offers better smoothing performance, but requires more work per iteration. In the following, we compare the computational work of these two methods and distributive relaxation.

5.3. *Comparing among* IBSR, *σ-Uzawa, and* DWJ *relaxation*

To end this section, we turn our attention to an estimate of the computational work for multigrid methods with σ-Uzawa, inexact Braess-Sarazin and distributive weighted-Jacobi relaxation. Since $\mu^2_{\text{opt},\sigma U} = \mu_{\text{opt},I}$, one cycle of multigrid with inexact Braess-Sarazin relaxation brings about the same total reduction in error as 2 cycles using σ-Uzawa relaxation. However, for inexact Braess-Sarazin and distributive weighted-Jacobi relaxation, $\mu_{\text{opt},I} = \mu_{\text{opt},D}$.

Considering the cost per sweep of inexact Braess-Sarazin relaxation and Uzawa relaxation, we see that inexact Braess-Sarazin is expected to be more efficient. Recall the inexact Braess-Sarazin relaxation (6), where $C = \text{diag}(A)$, requires inexact solution of

$$\begin{aligned} (BC^{-1}B^T)\delta p &= BC^{-1}r_{\mathcal{U}} - \alpha r_p, \\ \delta\mathcal{U} &= \frac{1}{\alpha}C^{-1}(r_{\mathcal{U}} - B^T\delta p). \end{aligned}$$

Since we use the standard finite-difference discretizations, C is just a diagonal matrix and C^{-1} is very simple to compute. For the first equation, we use a single sweep of weighted Jacobi iteration, having precomputed the approximate Schur complement, $B(C)^{-1}B^T$. Thus, the total cost of a single sweep of inexact BSR is that of 2 applications of C^{-1}, one sweep of weighted Jacobi for δp, one matrix-vector product each with B and B^T, and some vector updates. In σ-Uzawa relaxation, Equation (17) is equivalent to computing updates as

$$\begin{aligned} \delta\mathcal{U} &= (\alpha C)^{-1}r_{\mathcal{U}}, \\ S\delta p &= B\delta\mathcal{U} - r_p. \end{aligned}$$

Thus, the total cost of a single sweep is that of one application of C^{-1}, one diagonal scaling for δp, one matrix-vector product with B, and some vector updates. Thus, the cost of 2 sweeps of σ-Uzawa is slightly more than one sweep of inexact Braess-Sarazin and, in this case, inexact Braess-Sarazin is more efficient.

In distributive weighted-Jacobi relaxation, Equation (5) is equivalent to computing updates as

$$\begin{aligned} \delta\hat{\mathcal{U}} &= (\alpha C)^{-1}r_{\mathcal{U}}, \\ \delta\hat{p} &= \big(\alpha\text{diag}(A_p)\big)^{-1}(r_p - B\delta\hat{\mathcal{U}}), \end{aligned}$$

followed by distribution to the original unknowns by computing

$$\begin{aligned} \delta\mathcal{U} &= \delta\hat{\mathcal{U}} + B^T\delta\hat{p}, \\ \delta p &= -A_p\delta\hat{p}. \end{aligned}$$

Thus, the total cost of a single sweep is one application of $(\alpha C)^{-1}$, one sweep of Jacobi on A_p, one matrix-vector product with B^T and B, one application of A_p, and some vector updates. Comparing with inexact Braess-Sarazin relaxation, the cost of one sweep of distributive weighted-Jacobi relaxation is a slightly more than the cost of one sweep of inexact Braess-Sarazin relaxation.

DOI: 10.1002/nla

6. NUMERICAL EXPERIMENTS

In this section, we present the optimized smoothing and LFA two-grid convergence factors for distributive weighted-Jacobi, Braess-Sarazin-type, and Uzawa-type relaxation. Furthermore, we validate these predictions against measured multigrid convergence factors using distributive weighted-Jacobi, inexact Braess-Sarazin, and σ-Uzawa relaxations. The numerical results show good agreement between predicted convergence and the true performance, although some dependence is seen on the boundary conditions imposed, as noted elsewhere in the literature.

6.1. LFA spectral radius of error-propagation symbols

In this section, we show the spectral radius of the error-propagation symbol for distributive weighted-Jacobi, Braess-Sarazin, and Uzawa-type relaxation, computed with $h = \frac{1}{64}$. Figure 2 gives the spectral radius of the error-propagation symbol for DWJ as a function of $\boldsymbol{\theta}$, showing that distributive weighted-Jacobi relaxation reduces errors over the high frequencies quickly. Figure 3 displays these for exact BSR and IBSR, showing that both reduce the error over the high frequencies at a fast speed. Figure 4 displays these for Schur-Uzawa and σ-Uzawa. Here, we see very flat profiles in the upper right quadrant, particularly for the case of σ-Uzawa, which reduces the error at a much slower speed over the high frequencies.

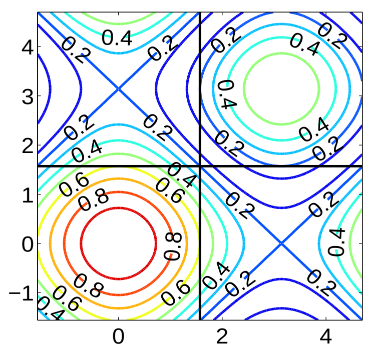

Figure 2. The spectral radius of the error-propagation symbol for DWJ, as a function of the Fourier mode, θ.

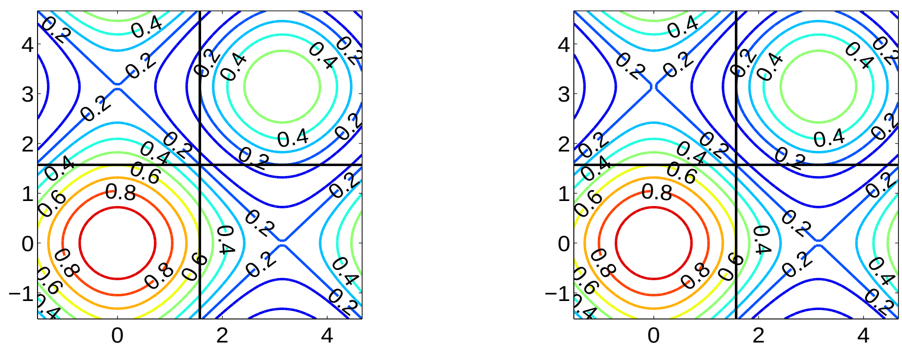

Figure 3. At left, the spectral radius of the error-propagation symbol for exact BSR, as a function of the Fourier mode, θ. At right, the spectral radius of the error-propagation symbol for inexact BSR.

DOI: 10.1002/nla

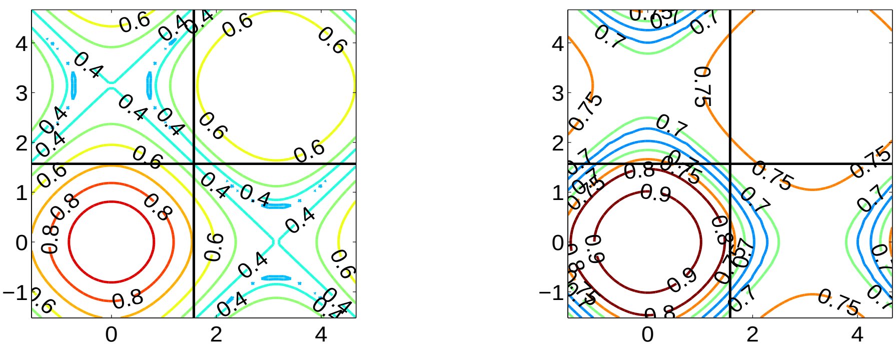

Figure 4. At left, the spectral radius of the error-propagation symbol for Schur-Uzawa, as a function of the Fourier mode, θ. At right, the spectral radius of the error-propagation symbol for σ-Uzawa.

6.2. *LFA two-grid convergence factor*

Let μ and ρ be the LFA-predicted smoothing and two-grid convergence factors, respectively, computed with $h = \frac{1}{64}$. For ρ, we first consider only one step of pre-smoothing (which gives the same results as one step of post-smoothing). At grid-points corresponding to velocity unknowns, u and v, we consider 6-point restrictions and at grid-points associated with pressure unknowns, p, a 4-point cell-centered restriction is applied. For the prolongation of the corrections, we apply the corresponding adjoint operators multiplied by a factor of 4 or bilinear interpolation for velocity (12pts) and pressure (16pts) see, e.g., [28]. In Table I, we give the choices of parameters for the relaxation schemes analyzed in the previous sections to present our LFA two-grid convergence factors. Note that parameter ω_J appears only in the IBSR algorithm, and σ only in σ-Uzawa.

Table I. Relaxation parameter choices

Relaxation / parameter	DWJ	BSR	IBSR	Schur-Uzawa	σ-Uzawa
ω	1	1	1	$\frac{4}{\sqrt{73}-3}$	1
α	$\frac{5}{4}\omega = \frac{5}{4}$	$\frac{5}{4}\omega = \frac{5}{4}$	$\frac{5}{4}$	$\frac{4}{\sqrt{73}-5}$	$\frac{5\omega^2}{5\omega-1} = \frac{5}{4}$
ω_J or σ	\	\	$\frac{4}{5}$	\	$\frac{1}{5\omega-1} = \frac{1}{4}$
μ_{opt}	$\frac{3}{5}$	$\frac{3}{5}$	$\frac{3}{5}$	$\sqrt{\frac{33-3\sqrt{73}}{41-3\sqrt{73}}}$	$\sqrt{\frac{3}{5}}$

Figures 5-9 show the spectra of the two-grid error-propagation operators for different relaxation methods. In Figure 5, both linear and bilinear interpolation result in the same convergence factor $\mu = 0.600$, which is equal to the optimal smoothing factor for DWJ. In Figure 5, we see many eigenvalues with linear interpolation cluster around zero compared with the bilinear case. This might indicate that the linear interpolation operator produces an algorithm that reduces the error better. In Figure 6, we again have $\rho = \mu$ for both linear and bilinear interpolation for exact Braess-Sarazin relaxation, with some complex eigenvalues for linear case, while all of the eigenvalues for bilinear interpolation are real. In Figure 7, we see some more significant difference between the distribution of the eigenvalues for the linear and bilinear cases, however the resulting spectral radii are the same. In Figure 8, for Schur Uzawa, we see that the two-grid spectral radius is larger than the smoothing factor with linear interpolation, but is the same as smoothing factor with bilinear interpolation. In Figure 9, both linear and bilinear interpolation for σ-Uzawa relaxation achieve the same convergence factor, $\rho = \sqrt{\frac{3}{5}}$, which is the same as the optimal smoothing factor, $\mu = \sqrt{\frac{3}{5}}$. All of these pictures confirm our theoretical optimal smoothing factors presented in previous sections, showing the (generally small) effect of the choice of interpolation.

DOI: 10.1002/nla

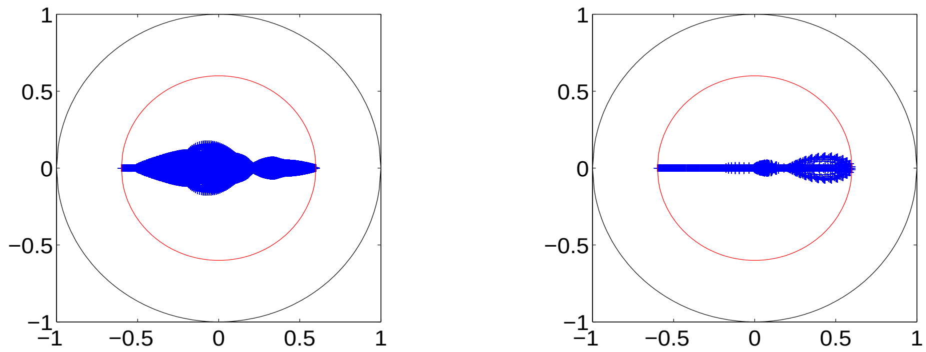

Figure 5. At left, the spectrum of the two-grid error-propagation operator for DWJ with linear interpolation. $\rho = \mu = 0.6000$. At right, the spectrum of the two-grid error-propagation operator for DWJ with bilinear interpolation. $\rho = \mu = 0.6000$.

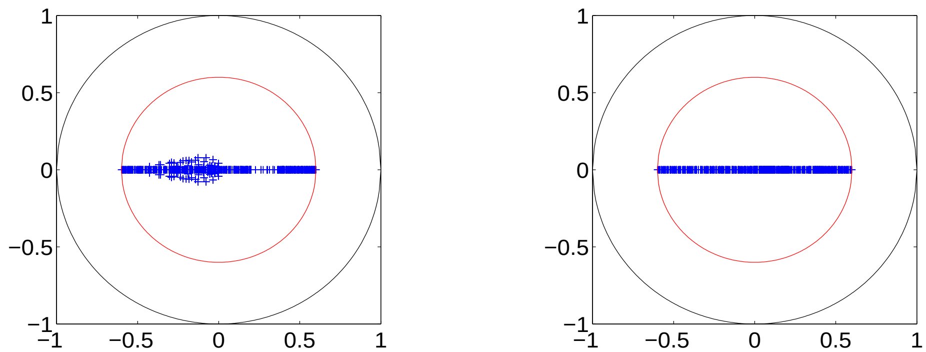

Figure 6. At left, the spectrum of the two-grid error-propagation operator for exact BSR with linear interpolation. $\rho = \mu = 0.6000$. At right, the spectrum of the two-grid error-propagation operator for exact BSR with bilinear interpolation. $\rho = \mu = 0.6000$.

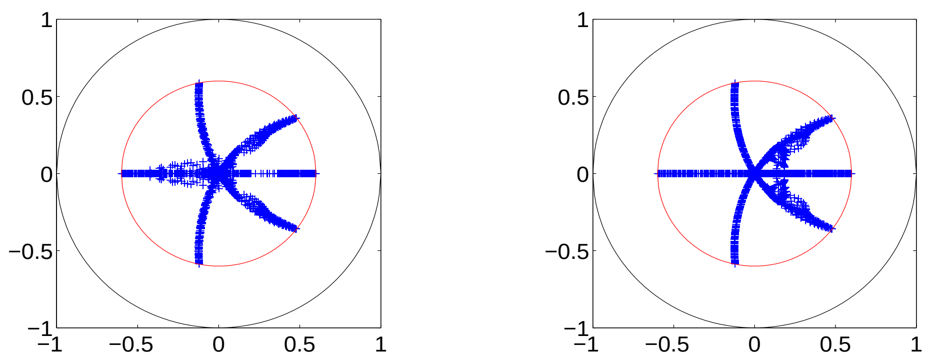

Figure 7. At left, the spectrum of the two-grid error-propagation operator for IBSR with linear interpolation. $\rho = \mu = 0.6000$. At right, the spectrum of the two-grid error-propagation operator for IBSR with bilinear interpolation. $\rho = \mu = 0.6000$.

DOI: 10.1002/nla

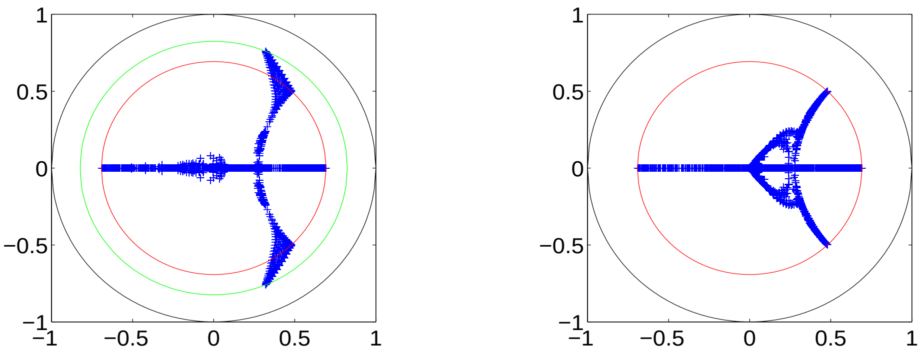

Figure 8. At left, the spectrum of the two-grid error-propagation operator for Schur-Uzawa with linear interpolation. $\rho = 0.8240, \mu = 0.6924$. At right, the spectrum of the two-grid error-propagation operator for Schur-Uzawa with bilinear interpolation. $\rho = \mu = 0.6924$.

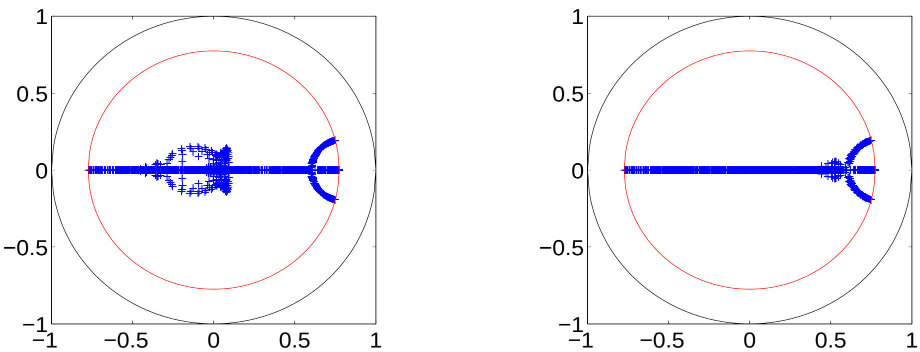

Figure 9. At left, the spectrum of the two-grid error-propagation operator for σ-Uzawa with linear interpolation. $\rho = \mu = \sqrt{\frac{3}{5}}$. At right, the spectrum of the two-grid error-propagation operator for σ-Uzawa with bilinear interpolation. $\rho = \mu = \sqrt{\frac{3}{5}}$

6.3. Multigrid convergence factor

We now validate our LFA results against measured multigrid performance. We use the notation $W(\nu_1, \nu_2)$ to indicate the cycle type and the number of pre- and postsmoothing steps employed. Here, we use the defects (full system residuals in (3)) $d_h^{(k)} (k = 1, 2, \cdots)$ to experimentally measure the convergence factor as $\hat{\rho}_h^{(k)} = \sqrt[k]{\frac{\|d_h^{(k)}\|_2}{\|d_h^{(0)}\|_2}}$ (see [30]), with $k = 100$. We consider the homogeneous problem ($b = 0$) with discrete solution $x_h \equiv 0$, and start with a random initial guess $x^{(0)}$ to test the multigrid convergence factor. The coarsest grid is a 4×4 mesh. Rediscretization is used to define the coarse-grid operator. For comparison, we present the LFA predicated convergence factors, ρ_h, for two-grid cycles with ν_1 prerelaxation and ν_2 postrelaxation steps.

In Table II, we present the multigrid performance of distributive weighted-Jacobi relaxation with Dirichlet boundary conditions. We see the same degradation in actual convergence behavior as was mentioned for distributive Gauss-Seidel in [28] and note that performance is h-independent. Furthermore, as we increase the number of relaxation sweeps, we see degradation in even the LFA-predication as compared to $\mu^{\nu_1+\nu_2}$ for bilinear interpolation. In order to see that boundary conditions play an important role in multigrid performance, we present the case of periodic boundary conditions in Table III. These results show measured multigrid convergence factors that coincide with the LFA-predicated convergence factors. Comparing linear and bilinear interpolation, these

Prepared using nlaauth.cls
DOI: 10.1002/nla

results indicate that linear interpolation outperforms bilinear interpolation in this case, matching some existing studies [8, 38, 39] for other relaxation schemes. Table IV shows that the measured multigrid convergence factors again match well with the LFA-predicted two-grid convergence factors for inexact Braess-Sarazin relaxation with Dirichlet boundary conditions, and that the convergence is h-independent. We note no major differences in results between linear and bilinear interpolation, except a small one (that is captured by the LFA) for $W(2,2)$ cycles. Similar results are seen with periodic boundary conditions.

For the σ-Uzawa relaxation, there are many choices for ω_U, α_U, and σ, see Theorem 5.4. We tested a range of parameter values for the multigrid method with Dirichlet boundary conditions, and found that the choice of $\omega_U = \frac{1}{5(2\sqrt{3/5}-1)}$ is typically best. Thus, we use this value in our numerical results. In Table V, the measured multigrid convergence factor degrades for $\nu_1+\nu_2>1$ for both linear and bilinear interpolation with Dirichlet boundary conditions, and the same behavior was seen using a two-grid method. To confirm this is due to LFA doing a poor job of capturing the effects of boundary conditions, we tested the σ-Uzawa relaxation with periodic boundary conditions. In Table VI, we see no major difference between the measured convergence using linear and bilinear interpolation with periodic boundary conditions, and good agreement between the LFA-predicted convergence factor and the measured multigrid convergence factor. Comparing Table VI with Table V, we conclude that the degradation seen in Table V is, in fact, due to boundary conditions.

Remark 6.1
We also tested the LFA-predicated two-grid convergence factors using Galerkin coarse-grid operators for the different relaxation schemes discussed in this paper. The convergence factors were almost the same as the ones obtained above using rediscretization coarse-grid operators for bilinear interpolation. However, for the case of linear interpolation, we see a large degradation in performance.

Remark 6.2
We see similar good performance for IBSR when using F-cycles; however, this is true only for Uzawa-type and distributive weighted-Jacobi relaxation on the problem with periodic boundary conditions. For $V(\nu_1,\nu_2)$-cycles with linear interpolation, when $\nu_1+\nu_2=1$, both Braess-Sarazin-type and Uzawa relaxations are divergent. However, when $\nu_1+\nu_2>1$, Braess-Sarazin relaxation works well for both Dirichlet and periodic boundary conditions, but Uzawa only works well for periodic boundary conditions. This is consistent with other studies of these relaxation schemes such as [20]. Distributive weighted-Jacobi relaxation has similar behavior as Braess-Sarazin relaxation. For $V(\nu_1,\nu_2)$-cycles with bilinear interpolation, all of these three relaxation schemes are convergent with both Dirichlet and periodic boundary conditions, although there is a different degradation for each case, compared with the LFA-predications.

Table II. Multigrid convergence factor for DWJ–Dirichlet BC

$\hat{\rho}_h$ \ Cycle	$W(0,1)$	$W(1,0)$	$W(1,1)$	$W(1,2)$	$W(2,1)$	$W(2,2)$
Linear interpolation						
$\rho_{h=1/256}$	0.600	0.600	0.360	0.216	0.216	0.130
$\hat{\rho}^{(100)}_{h=1/256}$	0.670	0.670	0.476	0.337	0.337	0.240
$\hat{\rho}^{(100)}_{h=1/128}$	0.673	0.672	0.475	0.338	0.337	0.240
Bilinear interpolation						
$\rho_{h=1/256}$	0.600	0.600	0.397	0.319	0.319	0.269
$\hat{\rho}^{(100)}_{h=1/256}$	0.668	0.668	0.474	0.340	0.340	0.270
$\hat{\rho}^{(100)}_{h=1/128}$	0.671	0.670	0.476	0.341	0.341	0.270

DOI: 10.1002/nla

Table III. Multigrid convergence factor for DWJ–Periodic BC

Cycle / $\hat{\rho}_h$	$W(0,1)$	$W(1,0)$	$W(1,1)$	$W(1,2)$	$W(2,1)$	$W(2,2)$
Linear interpolation						
$\rho_{h=1/256}$	0.600	0.600	0.360	0.216	0.216	0.130
$\hat{\rho}^{(100)}_{h=1/256}$	0.584	0.585	0.350	0.210	0.210	0.126
$\hat{\rho}^{(100)}_{h=1/128}$	0.584	0.585	0.350	0.211	0.210	0.127
Bilinear interpolation						
$\rho_{h=1/256}$	0.600	0.600	0.397	0.319	0.319	0.269
$\hat{\rho}^{(100)}_{h=1/256}$	0.584	0.584	0.381	0.303	0.302	0.253
$\hat{\rho}^{(100)}_{h=1/128}$	0.585	0.584	0.381	0.302	0.302	0.253

Table IV. Multigrid convergence factor for IBSR–Dirichlet BC

Cycle / $\hat{\rho}_h$	$W(0,1)$	$W(1,0)$	$W(1,1)$	$W(1,2)$	$W(2,1)$	$W(2,2)$
Linear interpolation						
$\rho_{h=1/256}$	0.600	0.600	0.360	0.216	0.216	0.130
$\hat{\rho}^{(100)}_{h=1/256}$	0.583	0.583	0.350	0.212	0.214	0.130
$\hat{\rho}^{(100)}_{h=1/128}$	0.583	0.582	0.350	0.214	0.213	0.130
Bilinear interpolation						
$\rho_{h=1/256}$	0.600	0.600	0.360	0.216	0.216	0.153
$\hat{\rho}^{(100)}_{h=1/256}$	0.582	0.581	0.349	0.209	0.209	0.146
$\hat{\rho}^{(100)}_{h=1/128}$	0.582	0.581	0.349	0.208	0.208	0.145

Table V. $\omega_U = \frac{1}{5(2\sqrt{3/5}-1)}$: Multigrid convergence factor for σ-Uzawa–Dirichlet BC

Cycle / $\hat{\rho}_h$	$W(0,1)$	$W(1,0)$	$W(1,1)$	$W(1,2)$	$W(2,1)$	$W(2,2)$
Linear interpolation						
$\rho_{h=1/256}$	0.775	0.775	0.600	0.465	0.465	0.360
$\hat{\rho}^{(100)}_{h=1/256}$	0.767	0.777	0.646	0.533	0.532	0.447
$\hat{\rho}^{(100)}_{h=1/128}$	0.780	0.783	0.646	0.540	0.538	0.450
Bilinear interpolation						
$\rho_{h=1/256}$	0.775	0.775	0.600	0.465	0.465	0.360
$\hat{\rho}^{(100)}_{h=1/256}$	0.775	0.778	0.644	0.534	0.534	0.445
$\hat{\rho}^{(100)}_{h=1/128}$	0.781	0.780	0.648	0.537	0.537	0.446

DOI: 10.1002/nla

Table VI. Multigrid convergence factor for σ-Uzawa–Periodic BC

Cycle / $\hat{\rho}_h$	$W(0,1)$	$W(1,0)$	$W(1,1)$	$W(1,2)$	$W(2,1)$	$W(2,2)$
Linear interpolation						
$\rho_{h=1/256}$	0.775	0.775	0.600	0.465	0.465	0.360
$\hat{\rho}^{(100)}_{h=1/256}$	0.752	0.752	0.580	0.449	0.449	0.347
$\hat{\rho}^{(100)}_{h=1/128}$	0.752	0.753	0.580	0.448	0.448	0.347
Bilinear interpolation						
$\rho_{h=1/256}$	0.775	0.775	0.600	0.465	0.465	0.360
$\hat{\rho}^{(100)}_{h=1/256}$	0.751	0.751	0.580	0.449	0.449	0.347
$\hat{\rho}^{(100)}_{h=1/128}$	0.753	0.751	0.579	0.448	0.448	0.347

7. CONCLUSION

In this paper, we develop a local Fourier analysis for block-structured relaxation schemes for the Stokes equations. The convergence and smoothing theorems presented here provide us with optimized parameters for distributive weighted-Jacobi, Braess-Sarazin, and Uzawa relaxation. From the theory, the inexact Braess-Sarazin method has been proven to be as good as the exact iteration for solving the Stokes equations, with certain choices of parameters, and the convergence of the distributive weighted-Jacobi relaxation is as good as Braess-Sarazin, but both outperform Uzawa. For implementation, we consider the inexact cases, with weighted Jacobi iterations, as is suitable for use on modern in parallel and GPU architectures. In practice, we see much less sensitivity to boundary conditions for IBSR and, hence, generally recommend this as most efficient and robust of the approaches considered. Overall, the analysis presented here gives good insight into the use of block-structured relaxation for other types of saddle-point problems. Developing LFA smoothing analysis to determine the optimal parameters in these relaxation schemes for finite-element discretization methods, for example, stable and stabilized rectangular elements for the Stokes Equation, will be a focus of our future research, as will be extensions to other saddle-point problems.

REFERENCES

1. Bank RE, Welfert BD, Yserentant H. A class of iterative methods for solving saddle point problems. *Numer. Math.* 1990; **56**(7):645–666, doi:10.1007/BF01405194.
2. Benzi M, Golub GH, Liesen J. Numerical solution of saddle point problems. *Acta Numer.* 2005; **14**:1–137, doi: 10.1017/S0962492904000212.
3. Elman HC, Silvester DJ, Wathen AJ. *Finite elements and fast iterative solvers: with applications in incompressible fluid dynamics*. Second edn., Numerical Mathematics and Scientific Computation, Oxford University Press, Oxford, 2014, doi:10.1093/acprof:oso/9780199678792.001.0001.
4. Ruge JW, Stüben K. Algebraic multigrid. *Multigrid methods* 1987; **3**(13):73–130.
5. Adler JH, Benson TR, MacLachlan SP. Preconditioning a mass-conserving discontinuous galerkin discretization of the stokes equations. *Numerical Linear Algebra with Applications* 2017; **24**(3):e2047–n/a, doi:10.1002/nla.2047. E2047 nla.2047.
6. Brandt A, Dinar N. Multigrid solutions to elliptic flow problems. *Numerical methods for partial differential equations (Proc. Adv. Sem., Math. Res. Center, Univ. Wisconsin, Madison, Wis., 1978)*, *Publ. Math. Res. Center Univ. Wisconsin*, vol. 42. Academic Press, New York-London, 1979; 53–147.
7. Wittum G. Multi-grid methods for Stokes and Navier-Stokes equations. *Numerische Mathematik* 1989; **54**(5):543–563.
8. Oosterlee CW, Gaspar FJ. Multigrid methods for the Stokes system. *Computing in Science & Engineering* 2006; **8**(6):34–43.
9. Vanka SP. Block-implicit multigrid solution of Navier-Stokes equations in primitive variables. *J. Comput. Phys.* 1986; **65**(1):138–158, doi:10.1016/0021-9991(86)90008-2.
10. Braess D, Sarazin R. An efficient smoother for the Stokes problem. *Appl. Numer. Math.* 1997; **23**(1):3–19.

11. Maitre JF, Musy F, Nigon P. A fast solver for the Stokes equations using multigrid with a Uzawa smoother. *Advances in multigrid methods (Oberwolfach, 1984)*, *Notes Numer. Fluid Mech.*, vol. 11. Vieweg, Braunschweig, 1985; 77–83.
12. Braess D, Dahmen W. A cascadic multigrid algorithm for the Stokes equations. *Numer. Math.* 1999; **82**(2):179–191, doi:10.1007/s002110050416.
13. Adler J, Benson TR, Cyr E, MacLachlan SP, Tuminaro RS. Monolithic multigrid methods for two-dimensional resistive magnetohydrodynamics. *SIAM J. Sci. Comput.* 2016; **38**(1):B1–B24.
14. Adler JH, Emerson DB, MacLachlan SP, Manteuffel TA. Constrained optimization for liquid crystal equilibria. *SIAM J. Sci. Comput.* 2016; **38**(1):B50–B76, doi:10.1137/141001846.
15. MacLachlan SP, Oosterlee CW. Local Fourier analysis for multigrid with overlapping smoothers applied to systems of PDEs. *Numer. Linear Algebra Appl.* 2011; **18**(4):751–774, doi:10.1002/nla.762.
16. Manservisi S. Numerical analysis of Vanka-type solvers for steady Stokes and Navier-Stokes flows. *SIAM J. Numer. Anal.* 2006; **44**(5):2025–2056, doi:10.1137/060655407.
17. Rodrigo C, Gaspar FJ, Lisbona FJ. On a local Fourier analysis for overlapping block smoothers on triangular grids. *Appl. Numer. Math.* 2016; **105**:96–111, doi:10.1016/j.apnum.2016.02.006.
18. Schöberl J, Zulehner W. On Schwarz-type smoothers for saddle point problems. *Numer. Math.* 2003; **95**(2):377–399, doi:10.1007/s00211-002-0448-3.
19. John L, Rüde U, Wohlmuth B, Zulehner W. On the analysis of block smoothers for saddle point problems. *arXiv preprint arXiv:1612.01333* 2016; .
20. Gaspar FJ, Notay Y, Oosterlee CW, Rodrigo C. A simple and efficient segregated smoother for the discrete Stokes equations. *SIAM J. Sci. Comput.* 2014; **36**(3):A1187–A1206, doi:10.1137/130920630.
21. Gmeiner B, Huber M, John L, Rüde U, Wohlmuth B. A quantitative performance analysis for Stokes solvers at the extreme scale. *arXiv preprint arXiv:1511.02134* 2015; .
22. Olshanskii MA. Multigrid analysis for the time dependent Stokes problem. *Math. Comp.* 2012; **81**(277):57–79, doi:10.1090/S0025-5718-2011-02494-4.
23. Bacuta C, Vassilevski PS, Zhang S. A new approach for solving Stokes systems arising from a distributive relaxation method. *Numerical Methods for Partial Differential Equations* 2011; **27**(4):898–914.
24. Wang M, Chen L. Multigrid methods for the Stokes equations using distributive Gauss-Seidel relaxations based on the least squares commutator. *J. Sci. Comput.* 2013; **56**(2):409–431, doi:10.1007/s10915-013-9684-1.
25. Chen L. Multigrid methods for saddle point systems using constrained smoothers. *Comput. Math. Appl.* 2015; **70**(12):2854–2866, doi:10.1016/j.camwa.2015.09.020.
26. Takacs S. A robust multigrid method for the time-dependent Stokes problem. *SIAM J. Numer. Anal.* 2015; **53**(6):2634–2654, doi:10.1137/140969658.
27. Zulehner W. A class of smoothers for saddle point problems. *Computing* 2000; **65**(3):227–246, doi:10.1007/s006070070008.
28. Niestegge A, Witsch K. Analysis of a multigrid Stokes solver. *Appl. Math. Comput.* 1990; **35**(3):291–303.
29. Luo P, Rodrigo C, Gaspar F, Oosterlee C. On an Uzawa smoother in multigrid for poroelasticity equations. *Numerical Linear Algebra with Applications* 2017; **24**(1).
30. Trottenberg U, Oosterlee CW, Schüller A. *Multigrid*. Academic Press, Inc., San Diego, CA, 2001. With contributions by A. Brandt, P. Oswald and K. Stüben.
31. Harlow FH, Welch JE. Numerical calculation of time-dependent viscous incompressible flow of fluid with free surface. *Physics of Fluids* 1965; **8**(12):2182–2189.
32. Chen L, Hu X, Wang M, Xu J. A multigrid solver based on distributive smoother and residual overweighting for Oseen problems. *Numerical Mathematics: Theory, Methods and Applications* 2015; **8**(02):237–252.
33. Gresho PM, Sani RL. On pressure boundary conditions for the incompressible Navier-Stokes equations. *International Journal for Numerical Methods in Fluids* 1987; **7**(10):1111–1145.
34. Keller C, Gould NIM, Wathen AJ. Constraint preconditioning for indefinite linear systems. *SIAM J. Matrix Anal. Appl.* 2000; **21**(4):1300–1317, doi:10.1137/S0895479899351805.
35. Larin M, Reusken A. A comparative study of efficient iterative solvers for generalized Stokes equations. *Numer. Linear Algebra Appl.* 2008; **15**(1):13–34, doi:10.1002/nla.561.
36. Elman HC, Golub GH. Inexact and preconditioned Uzawa algorithms for saddle point problems. *SIAM J. Numer. Anal.* 1994; **31**(6):1645–1661, doi:10.1137/0731085.
37. Bramble JH, Pasciak JE, Vassilev AT. Analysis of the inexact Uzawa algorithm for saddle point problems. *SIAM J. Numer. Anal.* 1997; **34**(3):1072–1092, doi:10.1137/S0036142994273343.
38. Wesseling P. *An introduction to multigrid methods*. Pure and Applied Mathematics (New York), John Wiley & Sons, Ltd., Chichester, 1992.
39. Wesseling P, Oosterlee CW. Geometric multigrid with applications to computational fluid dynamics. *Journal of Computational and Applied Mathematics* 2001; **128**(1):311–334.